Geochemistry Geophysics Geosystems G3
AN ELECTRONIC JOURNAL OF THE EARTH SCIENCES
Published by AGU and the Geochemical Society

Article
Volume 8, Number 8
4 August 2007
Q08002, doi:10.1029/2007GC001617
ISSN: 1525-2027

Hydrothermal alteration and microbial sulfate reduction in peridotite and gabbro exposed by detachment faulting at the Mid-Atlantic Ridge, 15°20′N (ODP Leg 209): A sulfur and oxygen isotope study

Jeffrey C. Alt
Department of Geological Sciences, University of Michigan, 2534 C.C. Little Building, Ann Arbor, Michigan 48109-1005, USA (jalt@umich.edu)

Wayne C. Shanks III
U. S. Geological Survey, Denver Federal Center, MS 973, Denver, Colorado 80225, USA (pshanks@usgs.gov)

Wolfgang Bach
Fachbereich 5 - Geowissenschaften, Universität Bremen, Postfach 33 04 40, D-28334 Bremen, Germany (wbach@uni-bremen.de)

Holger Paulick
Mineralogisch-Petrologisches Institut, Universität Bonn, Poppelsdorfer Schloss, D-53115 Bonn, Germany

Carlos J. Garrido
Departamento de Mineralogia y Petrologia Facultad de Ciencias, Fuentenueva s/n Universidad de Granada, E-18002 Granada, Spain

Georges Beaudoin
Département de Géologie et de Génie Géologique, Université Laval, Quebec, Quebec, Canada G1K 7P4 (beaudoin@ggl.ulaval.ca)

[1] Whole rock sulfur and oxygen isotope compositions of altered peridotites and gabbros from near the 15°20′N Fracture Zone on the Mid-Atlantic Ridge were analyzed to investigate hydrothermal alteration processes and test for a subsurface biosphere in oceanic basement. Three processes are identified. (1) High-temperature hydrothermal alteration (~250–350°C) at Sites 1268 and 1271 is characterized by ^{18}O depletion (2.6–4.4‰), elevated sulfide-S, and high $\delta^{34}S$ (up to ~2 wt% and 4.4–10.8‰). Fluids were derived from high-temperature (>350°C) reaction of seawater with gabbro at depth. These cores contain gabbroic rocks, suggesting that associated heat may influence serpentinization. (2) Low-temperature (<150°C) serpentinization at Sites 1272 and 1274 is characterized by elevated $\delta^{18}O$ (up to 8.1‰), high sulfide-S (up to ~3000 ppm), and negative $\delta^{34}S$ (to −32.1‰) that reflect microbial reduction of seawater sulfate. These holes penetrate faults at depth, suggesting links between faulting and temperatures of serpentinization. (3) Late low-temperature oxidation of sulfide minerals caused loss of sulfur from rocks close to the seafloor. Sulfate at all sites contains a component of oxidized sulfide minerals. Low $\delta^{34}S$ of sulfate may result from kinetic isotope fractionation during oxidation or may indicate readily oxidized low-$\delta^{34}S$ sulfide derived from microbial sulfate reduction. Results show that peridotite alteration may be commonly affected by fluids ± heat derived from mafic intrusions and that microbial sulfate reduction is widespread in mantle exposed at the seafloor.

Components: 11,841 words, 9 figures, 2 tables.

Keywords: stable isotopes; biosphere; mid-ocean ridges; hydrothermal systems; geochemistry.

Index Terms: 1041 Geochemistry: Stable isotope geochemistry (0454, 4870); 1034 Geochemistry: Hydrothermal systems (0450, 3017, 3616, 4832, 8135, 8424); 1032 Geochemistry: Mid-oceanic ridge processes (3614, 8416).

Received 21 February 2007; **Revised** 14 May 2007; **Accepted** 18 May 2007; **Published** 4 August 2007.

Alt, J. C., W. C. Shanks III, W. Bach, H. Paulick, C. J. Garrido, and G. Beaudoin (2007), Hydrothermal alteration and microbial sulfate reduction in peridotite and gabbro exposed by detachment faulting at the Mid-Atlantic Ridge, 15°20′N (ODP Leg 209): A sulfur and oxygen isotope study, *Geochem. Geophys. Geosyst.*, *8*, Q08002, doi:10.1029/2007GC001617.

1. Introduction

[2] Mantle peridotites are commonly exposed in oceanic fracture zones and along low-angle faults related to tectonic extension and crustal thinning at slow-spreading mid-ocean ridges [e.g., *Escartín et al.*, 2003; *Mevel*, 2003]. Approximately half of the global mid-ocean ridge system spreads at slow rates (<40 mm y^{-1} [*Carbotte and Scheirer*, 2004]), so peridotites are an integral part of the upper oceanic crust, and seawater interaction with these rocks at various conditions is important for the evolution of the lithosphere. Different approaches are important for understanding serpentinization of oceanic peridotites [e.g., *Moody*, 1976; *Douville et al.*, 2002; *Allen and Seyfried*, 2003, 2004; *Bach et al.*, 2004a; *Palandri and Reed*, 2004; *Seyfried et al.*, 2004; *Barnes and Sharp*, 2006; *Paulick et al.*, 2006]. In particular, oxygen and sulfur isotope geochemistry have been shown to be especially useful for documenting temperatures and identifying microbial processes during serpentinization [e.g., *Agrinier et al.*, 1995, 1996; *Fruh-Green et al.*, 1996; *Alt and Shanks*, 1998, 2003]. The mineralogy and chemistry of oceanic serpentinites and the physical and chemical processes attending serpentinization have been summarized in recent reviews [*Mevel*, 2003; *Seyfried et al.*, 2004], which document a wide range of serpentinization temperatures, from ~500°C down to ambient seafloor conditions (near 0°C). The focus of this paper is on sulfur and oxygen isotopes, so results from sites where both oxygen and sulfur isotope studies have been carried out are briefly summarized below in order to illustrate the range of processes previously documented.

[3] Fluid circulation and serpentinization of oceanic peridotites at high temperatures is driven by heat supplied either by cooling of ultramafic lithosphere or by intrusion of mafic magma into peridotite. At Hess Deep, oxygen isotope data indicate that serpentinization of the upper mantle took place at temperatures of 275–375°C as seawater penetrated downward during rifting related to propagation of the Galapagos spreading center [*Agrinier et al.*, 1995; *Fruh-Green et al.*, 1996]. Here, low seawater-rock ratios resulted in strongly reducing conditions, formation of a low-sulfur secondary mineral assemblage, and little change in bulk rock S contents or isotope compositions [*Alt and Shanks*, 1998]. On the MAR (Mid-Atlantic Ridge), high-temperature (~360°C) black smokers at the Logatchev (at 14°45′N) and Rainbow (36°14′N) hydrothermal sites are located on peridotite and reflect reactions of seawater with peridotite at depth, although whether there is a magmatic heat contribution is unclear [*Douville et al.*, 2002; *Allen and Seyfried*, 2003]. At the MARK area on the MAR, serpentinization of peridotites occurred via hydrothermal fluids derived from prior seawater interactions with gabbros at temperatures above ~350°C, leading to highly elevated S contents and $\delta^{34}S$ values in the serpentinites (up to 1 wt% S, and $\delta^{34}S$ ~7‰ [*Alt and Shanks*, 2003]). Massive sulfide breccias sampled from ultramafic material on the Southwest Indian Ridge similarly may be derived from high temperature serpentinization reactions at depth, indicating significant mass transport of sulfur and metals associated with serpentinization [*Bach et al.*, 2002].

[4] Lower-temperature reactions associated with serpentinization can support microbial activity within the rocks and at sites of fluid venting [*Alt and Shanks*, 1998; *Kelley et al.*, 2001, 2005]. At the Iberian margin, oxygen isotope data indicate that peridotites exposed by tectonic extension during opening of the Atlantic were serpentinized at relatively low temperatures (~0–150°C [*Agrinier et al.*, 1996]). Serpentinization reactions generated hydrogen, which supported microbial communities

including sulfate reducers and methanogens, leading to addition of significant amounts of microbially generated sulfide (up to 0.4 wt% S, δ^{34}S down to −43‰) to the rocks and to methane anomalies in pore waters of overlying sediments [*Alt and Shanks*, 1998]. These inferences from the geochemistry of serpentinites were later confirmed by discovery of low-temperature (50–90°C) vents in serpentinite at the off-axis Lost City hydrothermal site near the Mid-Atlantic Ridge (MAR) [*Kelley et al.*, 2001, 2005]. Here, low sulfate concentration and elevated hydrogen and methane contents of fluids, the presence of sulfate reducers and methanogens, and hydrogen isotope data for fluids all indicate relatively low-temperature (<200°C) serpentinization reactions and significant microbial activity [*Allen and Seyfried*, 2004; *Kelley et al.*, 2005; *Proskurowski et al.*, 2006].

[5] Peridotites and gabbros are exposed in the area around the 15°20′N Fracture Zone (FZ) on the MAR [*Kelemen et al.*, 2004], and the rocks were affected by a range of alteration processes [e.g., *Bach et al.*, 2004a; *Paulick et al.*, 2006]. In this paper we present bulk rock sulfur and oxygen isotope analyses along with S contents and opaque mineral petrography of serpentinized peridotites and hydrothermally altered gabbros cored from this area by the Ocean Drilling Program (ODP). The objectives include a further understanding of hydrothermal processes affecting these peridotites, and how these processes vary from site to site. Understanding the variability of hydrothermal processes and the distribution of alteration effects is essential in order to ultimately quantify heat and mass transport in submarine hydrothermal systems. Of particular interest in this study is determining whether biotic activity as documented by microbial sulfate reduction during serpentinization has taken place, and how this may relate to other alteration processes, with the overarching goal of understanding the extent of the subsurface biosphere in oceanic lithosphere.

2. Geological Setting and Samples

[6] The area of the 15°20′N FZ on the MAR has been well-studied by geophysical, dredging, and submersible surveys [see *Escartín et al.*, 2003; *Kelemen et al.*, 2004]. Mantle peridotites and lower crustal gabbros are exposed on both flanks of the MAR to the north and south of the fracture zone. These oceanic core complexes formed by crustal thinning along long-lived low-angle detachment faults. Active hydrothermal venting is common in the area as indicated by strong methane and hydrogen anomalies in the water column [*Bougault et al.*, 1993; *Charlou et al.*, 1998], and by the presence of high-temperature hydrothermal vents within faulted serpentinite at the Logatchev site (Figure 1).

[7] Several sites were cored during ODP Leg 209, and these sites and the recovered rocks are described in detail by *Kelemen et al.* [2004]. Mantle peridotites from Leg 209 (Site 1274) are highly depleted, in terms of lacking residual clinopyroxene, olivine Mg# (up to 0.92) and spinel Cr# (∼0.5), suggesting a high degree of partial melting (>20% [*Seyler et al.*, 2007]). Petrographic descriptions of serpentinization and discussion of hydrothermal and serpentinization processes are given by *Bach et al.* [2004a, 2006], and the whole rock geochemistry of altered peridotites is presented by *Paulick et al.* [2006]. The drill sites and samples for this study are briefly summarized below on the basis of these previous studies.

2.1. Site 1268

[8] Hole 1268A is located on the western rift valley wall, south of the 15°20′ FZ (Figure 1). The hole penetrates 147.6 m into completely altered harzburgite and dunite, with local mylonitic shear zones, and highly altered late-magmatic dikes (Figure 2). The lower portion of the hole is dominated by pervasively altered gabbronorite bodies. Pyroxenes in the gabbronorites are replaced by talc and chlorite, and plagioclase by chlorite and quartz [*Kelemen et al.*, 2004; *Bach et al.*, 2004a]. Peridotites were altered in two general stages: initial serpentinization resulted in formation of serpentine + magnetite ± pyrite in the rocks, and a later stage of talc alteration resulted in replacement of serpentine by talc.

2.2. Site 1270

[9] Four shallow holes (18–57 m deep) were drilled at Site 1270 on the eastern rift valley wall (Figure 1). Holes 1270C and D are adjacent to each other, whereas Holes 1270A and B lie ∼300 m and 500 m downslope to the west, respectively [*Kelemen et al.*, 2004]. Holes 1270A, C, and D consist of harzburgite and dunite altered to serpentine + magnetite. Less serpentinized areas containing relict olivine and orthopyroxene, with orthopyroxene partly altered to talc and tremolite, provide evidence for high temperature (>350°C to 400°C) alteration [*Bach et al.*, 2004a]. Hole 1270D also recovered local sheared and hydrothermally altered

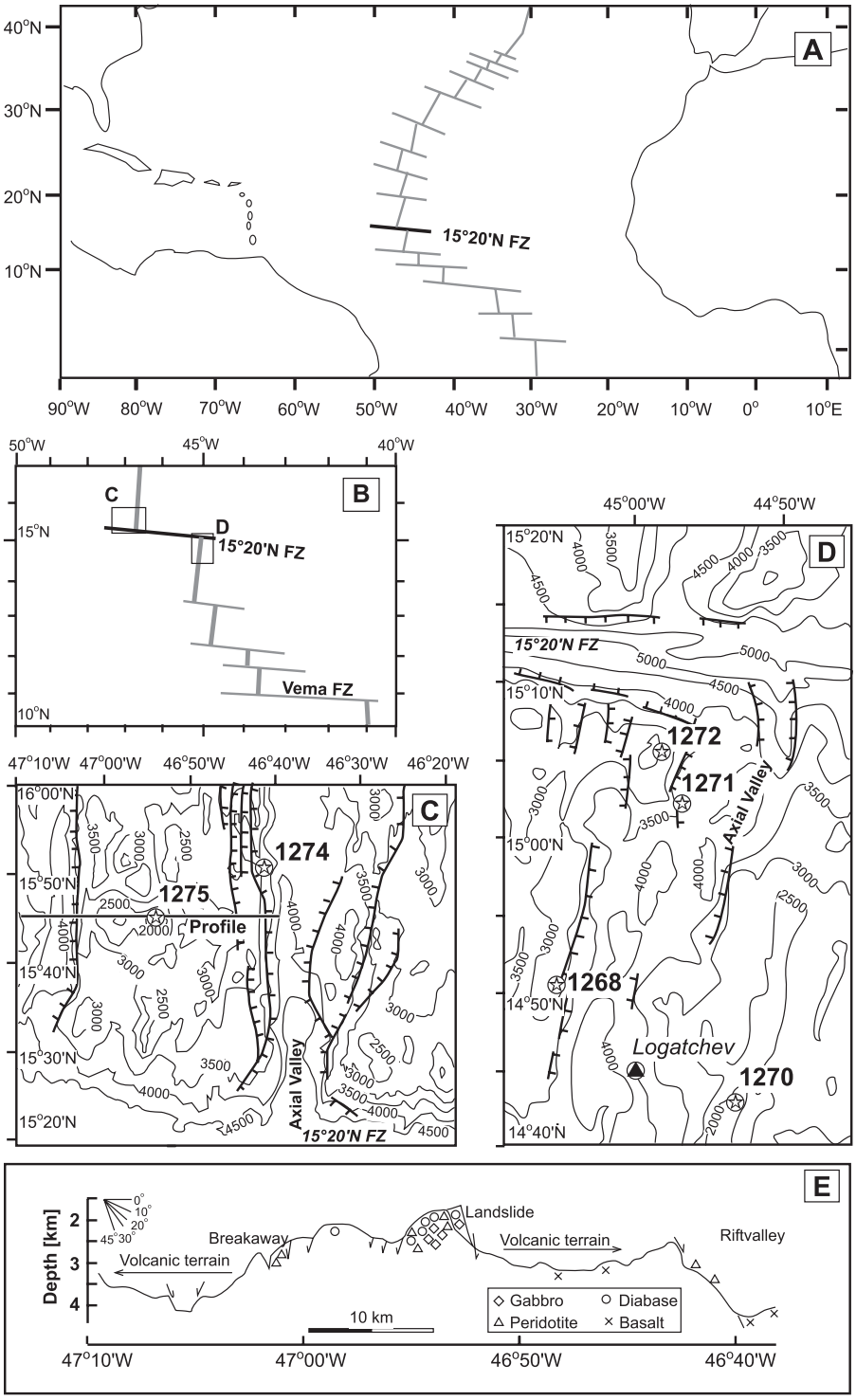

Figure 1. Locations of ODP Leg 209 drill holes near the 15°20′N Fracture Zone and the Mid-Atlantic Ridge. (a) Location of the 15°20′N Fracture Zone in the Atlantic Ocean. (b) Location of the southern and northern working area of ODP Leg 209. (c and d) Location of ODP sites 1268, 1270, 1271, 1272, 1274, and 1275 (stars). The location of the Logatchev active hydrothermal site (triangle) is also shown. Bathymetry of Figure 1c from *Fujiwara et al.* [2003]. Bathymetry of Figure 1d from *Lagabrielle et al.* [1998]. (e) Profile along section marked in Figure 1c which includes ODP site 1275 located on the top of a megamullion structure (modified from *Escartín et al.* [2003]). Sampling of the seafloor shows that this area is dominated by mafic and ultramafic plutonic rocks whereas volcanic terrains are located to the east and west of this elevated structure. Figure modified from *Paulick et al.* [2006] with permission from Elsevier.

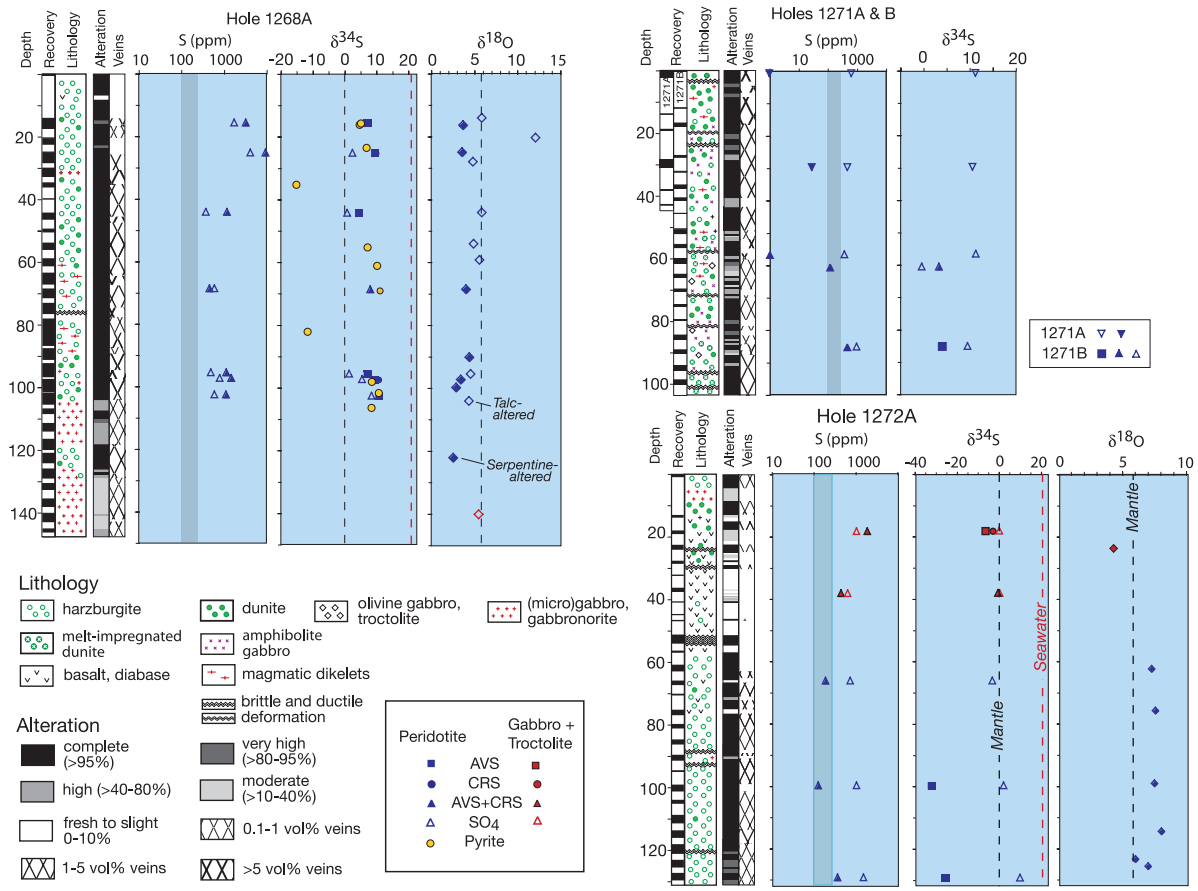

Figure 2. Lithostratigraphy and sulfur and oxygen isotope data for Leg 209 drill sites. AVS, acid-volatile sulfide; CRS, chrome-reduced sulfide; SO_4, sulfate-sulfur; Pyrite, vein pyrite (see text for further explanation). Shaded band indicates range of sulfur contents for fertile and depleted mantle (250–100 ppm). Dashed lines indicate S and O isotope compositions of mantle and S isotope composition of seawater. Lithology, percent core recovery, and alteration from *Kelemen et al.* [2004].

gabbroic material. Minor veins of carbonates and Fe-oxyhydroxides are the result of low-temperature alteration near the seafloor. Hole 1270B penetrates 46 m into gabbros and gabbronorites with traces of completely altered peridotites. The gabbroic rocks are weakly hydrothermally altered under static conditions, with formation of chlorite plus dark green and rare brown amphibole along grain boundaries.

2.3. Site 1271

[10] Two holes were drilled at Site 1271, located on the inside corner high of the spreading segment south of the 15°20′ FZ (Figure 1). Hole 1271A penetrates 44.8 m, recovering predominantly dunite that is completely altered to serpentine + magnetite, with local brucite (Figure 2). Some intervals exhibit effects of low-temperature seafloor alteration and oxidation (Fe-oxyhydroxides). Hole 1271B extends 103.6 m into a complex association of mafic rocks and variably altered dunite and lesser harzburgite. Below ~50 mbsf, mafic melts intruded and infiltrated the ultramafic rocks, and experienced syn-deformational hydrothermal alteration to amphibolite. Dunites associated with amphibolite are generally less altered than elsewhere in the core. Amphibole is pseudomorphic after olivine and talc replaces orthopyroxene in ultramafic rocks associated with amphibolite.

2.4. Site 1272

[11] Hole 1272A is located on the western flank of the Mid-Atlantic rift valley just south of the 15°20′ FZ (Figure 1). The hole penetrates 131 m (Figure 2), the upper ~50 m of which is a tectonic megabreccia consisting of diabase, vesicular basalt,

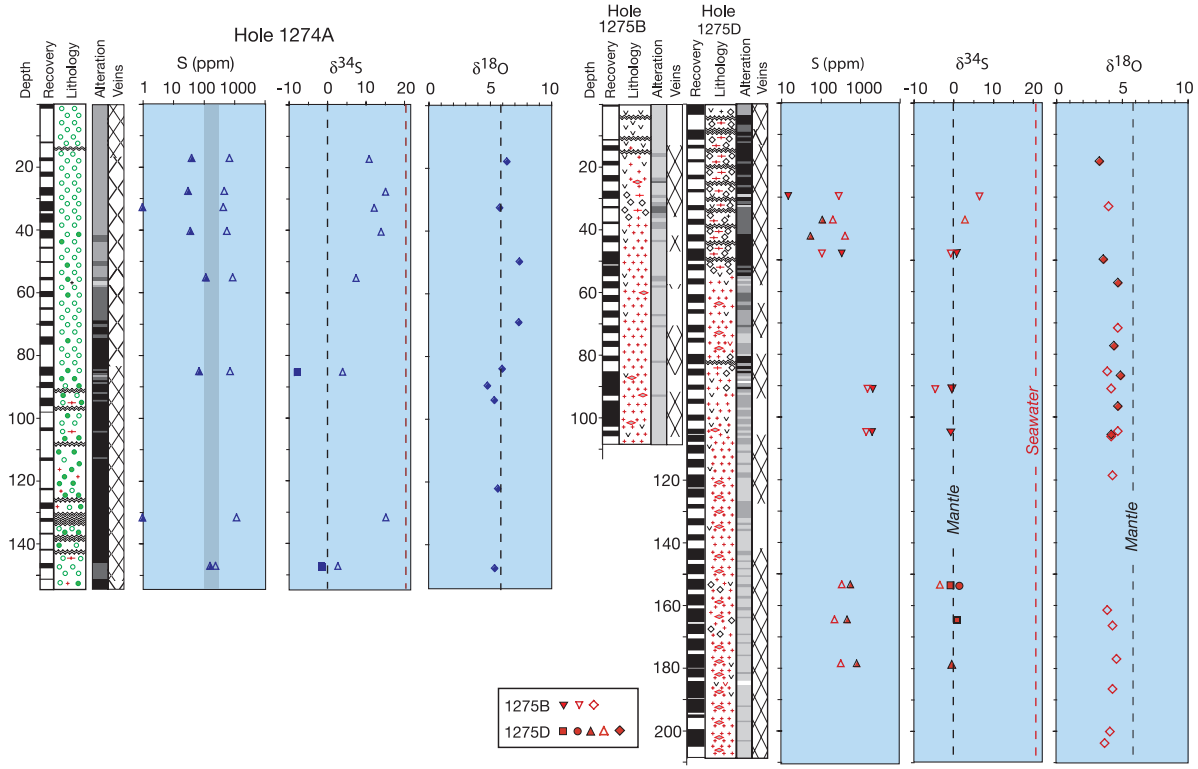

Figure 2. (continued)

gabbro, serpentinized peridotite and carbonate-cemented breccia with serpentinite clasts. In the upper 30 m oxidation of serpentinite to reddish brown clay, carbonate, and Fe-oxyhydroxide is abundant, especially associated with carbonate-clay cemented fault breccias. Below a fault gouge at 55 m the core consists of serpentinized harzburgite with minor dunite, containing assemblages of serpentine + magnetite ± brucite ± iowaite. Iowaite is common and formed from Fe-bearing brucite during late-stage low-temperature oxidizing alteration [*Bach et al.*, 2004a].

2.5. Site 1274

[12] Hole 1274A lies on the western flank of the Mid-Atlantic rift valley, north of the 15°20′ FZ (Figure 1), and penetrates 156 m into harzburgites and dunites (Figure 2). Rocks from Hole 1274A are the least altered rocks from Leg 209, but nevertheless range from highly altered (~60 vol% secondary minerals) in the upper half of the hole to completely altered (>95% secondary minerals) in the lower half, where abundant fault zones occur. Brucite + serpentine + magnetite characterize alteration of dunite, but brucite is rare in harzburgite. The upper 90 m of the hole has been affected by oxidative seawater alteration, characterized by cm-wide Fe-oxyhydroxide bearing alteration halos along carbonate veins.

2.6. Site 1275

[13] Site 1275 is sited atop a megamullion dome ~18 km west of the Mid-Atlantic rift valley at ~15°44′N (Figure 1). Hole 1275B penetrated 109 m into gabbroic rocks and minor troctolite (Figure 2). Diabase also occurs in the upper 15 m and in small amounts throughout the core. Hole 1275D, 90 m to the south of 1275B, extends to 209 m: the upper 56 m and an interval at 80–95 mbsf are dominated by troctolite whereas the remainder consists mainly of gabbroic rocks.

[14] The troctolites are highly altered to serpentine, magnetite, chlorite, and local talc and amphibole. The gabbroic section is weakly altered and shows no systematic variation with depth or deformation. Gabbroic rocks exhibit variable static alteration at amphibolite to greenschist facies conditions, characterized by formation of green amphibole and chlorite along grain boundaries. Dark green amphibole veins locally cut high-temperature foliation and intrusive contacts. Minor amounts of lower-

grade clays, iron-oxyhydroxides, and carbonates are present in rocks and veins.

3. Methods

[15] Samples selected for this study are a subset of those analyzed for bulk rock chemistry by *Paulick et al.* [2006], and are representative of rock and alteration types recovered in Leg 209 drill cores. Acid-volatile sulfide (AVS) was extracted in HCl under N_2 atmosphere with $SnCl_2$ added to prevent oxidation, and pyrite sulfur (CRS) was extracted using the Cr-reduction method [*Canfield et al.*, 1986; *Rice et al.*, 1993] at the University of Michigan. H_2S evolved from sulfide minerals was precipitated as Ag_2S and soluble sulfate reduced to H_2S by reaction with Thode's solution (HI + H_3PO_2 + HCl). For several samples where sulfide-S from the AVS extraction step was insufficient (<1 mg Ag_2S), this was combined with the CRS for determination of sulfide-S content and $\delta^{34}S$. The precipitates were combusted using an elemental analyzer interfaced directly in continuous flow mode to a Micromass Optima mass spectrometer in the U.S. Geological Survey stable isotope laboratory in Denver, CO. Sulfur isotope values are reported as standard δ notation relative to CDT where IAEA-S-1 = −0.30 per mil and IAEA-S-2 = 22.67 vs. CDT [*Coplen and Krouse*, 1998], with a precision better than ±0.2‰. Replicate extractions and analyses of bulk samples were reproducible within 0.5‰. Opaque mineralogy and petrography were determined by reflected light microscopy and by scanning electron microscopy (SEM) using a Zeiss FEG-SEM equipped with energy dispersive X-ray analysis at Universidad de Granada (Spain).

[16] Whole rock powders of peridotites were reacted with BrF_5 using the method of *Clayton and Mayeda* [1963] at the stable isotope laboratory of Université Laval (Canada). Oxygen isotope ratios were determined by gas source mass spectrometry at the G.G. Hatch Stable Isotope Laboratory of the University of Ottawa and are reported in δ-notation relative to *V*-SMOW where NBS-28 has value of 9.6‰, with a precision better than ±0.2‰.

[17] In addition, laser fluorination analyses of gabbro bulk rock powders were performed at the isotope laboratory of the University of Göttingen (Germany) applying analytical principles first described by *Sharp* [1990] and *Mattey and Macpherson* [1993]. Each analysis was made on 1.5 to 2 mg of sample powder by laser heating using a Synrad CO_2 laser in a fluorine gas atmosphere. The liberated O_2 was fixed on a microsieve and then released to an isotope-ratio-GCMS (irm GCMS). This setup consists of a Finnigan-MAT-Deltaplus gas ratio mass spectrometer, a Hewlett Packard 5890 gas chromatograph, and a Finnigan GC II interface. Duplicate analyses and analyses of in-house reference material (garnet UWG-2 [*Valley et al.*, 1995]) show that the reproducibility is better than ±0.2‰.

4. Results

4.1. Sulfur

[18] Serpentinized and altered peridotites and gabbros from the 15°20′N area have widely scattered S contents and $\delta^{34}S$ values (Table 1). The serpentinites exhibit variable enrichments and depletions of S and ^{34}S compared to fertile mantle values of ∼250 ppm and ∼0‰ (Figure 3). Several features of the data stand out in Figures 2 and 3, however. (1) Serpentinites from Holes 1272A and 1274A (and 2 pyrite veins from Hole 1268A) have negative $\delta^{34}S_{sulfide}$ values (down to −32‰; Figure 3b). (2) Sulfate at all sites has generally low $\delta^{34}S$ values (−4.5 to 15.3‰) compared to seawater sulfate (Figure 3c). The latter has a traditionally reported $\delta^{34}S$ value of 21‰ [*Rees et al.*, 1978], but recent corrections to the VCDT standard give a revised value of 22.6‰ [*Ding et al.*, 2001; *Davis et al.*, 2003]. (3) Hole 1268A rocks have high S contents and $\delta^{34}S_{sulfide}$ values (up to 1.3 wt% total S, and mostly ∼5–11‰, respectively). (4) Rocks from Sites 1270 and 1271 generally have very low sulfide-S contents. (5) Finally, gabbroic rocks from Site 1275 have widely varying sulfide-S contents (15–2110 ppm) and $\delta^{34}S_{sulfide}$ values that scatter about the mantle value of ∼0‰.

4.2. Oxygen Isotopes

[19] Serpentinized and talc-altered peridotites exhibit a wide range in whole rock $\delta^{18}O$ values, from 2.6 to 12.1‰ (Figure 4; Table 2), both enriched and depleted in ^{18}O relative to pristine mantle peridotite (5.5 ± 0.2‰ [*Mattey et al.*, 1994]). Some generalizations, however, can be made about the different sites. With the exception of three samples from Hole 1268A (having $\delta^{18}O$ values of 5.9–12.1‰), 18 altered peridotites from Sites 1268 and 1270 have low $\delta^{18}O$ values of 2.6–5.2‰ (Figure 4). Nine serpentinized harzburgites and dunites from Hole 1274A have $\delta^{18}O$ values of 4.8–7.4‰ that scatter about the mantle value.

Table 1. Whole Rock Sulfur Isotope and Sulfur Concentration Data for Leg 209 Rocks[a]

Sample	Rock Type	XRD Major/Minor/Trace	Depth, mbsf	S Content, ppm					δ^{34}S, ‰ CDT				
				AVS	CRS	AVS + CRS	SO4-S	Total S[b]	Py	AVS	CRS	AVS + CRS	SO_4
1268A 2R2 27-35	Harz	Serp/Talc/Mt	15.7	729	2539	3269	1735	4996		7.1	5.9		
1268A 4R1 44-55	Harz	Serp/Talc/	25.2	2132	7289	9421	4195	12533		9.5	9.8		2.5
1268A 8R1 28-35	Harz	Talc//	44.3	1179	0	1179	377	1155		4.4			0.9
1268A 13R1 46-55	Harz	Serp/Talc/	68.7			460	601	8241				8.1	
1268A 18R3 100-110	Harz	Talc//Serp	95.6	465	669	1134	494	1356		7.1	7.0		1.5
1268A 19R1 34-43	Harz	Serp//Talc	97.3	854	635	1489	802	1521		9.4	10.6		5.5
1268A 20R1 100-110	Harz	Serp//Mt	102.6	740	370	1110	600	1328		10.8	10.7		8.5
1268A 2R1 54-59	vein pyrite		16.1						4.6				
1268A 2R2 35-40	vein pyrite		15.7						5.0				
1268A 3R3 33-35	vein pyrite		23.42						6.8				
1268A 6R1 82-87	vein pyrite		35.22						−15.2				
1268A 10R2 10-13	vein pyrite		55.14						7.1				
1268A 11R2 102-105	vein pyrite		61.08						10.1				
1268A 13R1 99-104	vein pyrite		69.0						11.0				
1268A 15R4 11-15	vein pyrite		82.01						−11.7				
1268A 19R1 96-100	vein pyrite		97.96						8.4				
1268A 20R1 8-12	vein pyrite		101.6						10.5				
1268A 20R3 84-89	vein pyrite		106.29						8.3				
1270A 1R1 120-128	Harz	Serp//Mt	1.2	0	0	0	728	215					11.3
1270D 3R2 39-47	Harz	Serp/Talc/Mt	20.6	19	0	19	199	334					4.0
1271A 1R1 77-87	dunite	Serp/Mt/	0.8	0	0	0	716	228					11.3
1271A 4R2 5-15	dunite	Serp, Bru/Mt/	29.8	32	0	32	531	207					10.7
1271B 11R1 113-121	dunite	Serp//Mt	56.6	0	0	0	418	139					11.3
1271B 12R1 46-54	olivine gabbro	Serp/Amp, Ol/Mt, Bru	60.6			131	138	174				3.3	−0.4
1271B 17R1 61-69	dunite	Serp/Bru, Mt	85.1	496	0	496	1103	1000		4.0			9.6
1271B 17R1 8-15	gabbro	Pl, Amp/Chl/	84.6					20					
1272A 3R1 28-38	olivine gabbro	Pl/Amp, Qz/	18.2	645	1337	1983	1103	2723		−6.5	−3.1		0.2
1272A 7R1 116-124	diabase	Pl/Cpx	38.1			464	679	731				−0.3	0.3
1272A 14R1 43-53	Harz	Serp//Iwa	66.1	0	198	198	772	845					−3.0
1272A 21R1 88-100	Harz	Serp, Iwa//	99.8	134	0	134	1106	666		−32.1			2.3
1272A 27R2 78-88	Harz	Serp/Iwa/Bru	129.3	386	0	386	1616	1183		−25.5			10.2
1274A 3R1 61-71	Harz	Serp/Ol, Bru/Mt	17.5	41	0	41	720	348					10.9
1274A 5R2 25-35	Harz	Serp/Opx/Bru	28.0	31	0	31	482	152					15.2
1274A 6R3 24-34	Harz	Serp/Opx, Ol, Bru/	33.1	0	0	0	444	39					12.3
1274A 8R1 72-82	dunite	Serp/Bru/Ol	40.7	37	0	37	582	344					14.0
1274A 11R1 56-65	Harz	Serp//Bru, Ol	55.5	120	0	120	915	190					7.5
1274A 16R2 26-38	dunite	Serp//Bru, Mt, Iwa	85.4	71	0	71	749	410		−7.9			4.0
1274A 24R1 16-26	fault gouge	Serp/Mt/	132.0	0	0	0	1226	788					15.3
1274A 27R1 130-140	Harz	Serp/Opx, Ol, Bru/Mt	147.4	164	0	164	253	430		−1.5			2.8
1275B 3R1 26-33	diabase	Pl/Amp.Qz/	13.3					104					
1275B 6R2 85-93	troct	Serp/Talc, Chl/Ol	29.9	15	0	15	289	106					6.6
1275B 9R2 48-57	gabbro	Pl/Amp, Ilm/	43.6					40					

Table 1. (continued)

Sample	Rock Type	XRD Major/Minor/Trace	Depth, mbsf	S Content, ppm AVS	CRS	AVS + CRS	SO4-S	Total S[b]	δ^{34}S, ‰ CDT Py	AVS	CRS	AVS + CRS	SO_4
1275B 10R1 137-148	gabbro	Pl, Amp/Chl/Ilm	48.2			343	110	413				0.9	−0.6
1275B 19R2 45-56	gabbro	Pl/Amp, Cpx/Ilm	91.3	1736	375	2111	1548	3550			−0.5		−4.5
1275B 22R1 108-118	gabbro	Pl/Amp, Cpx/Ilm	105.1			2016	1444	1964				−0.6	
1275D 8R1 73-81	troct	Talc, Serp, Cc, Amp//	37.3			111	204	54					2.9
1275D 9R1 92-100	troct	Serp/Talc, Chl/	42.5	55	0	55	420	62					
1275D 33R2 80-90	micro-gabbro	Pl/Amp, Cpx/	153.5	532	34	566	347	661		−0.7	1.3		−3.4
1275D 35R4 28-35	micro-gabbro	Pl/Amp, Cpx, Chl/	164.7	468	0	468	228	191		0.9			
1275D 38R3 64-74	gabbro	Pl/Amp, Cpx/	178.7			822	327	492				−0.5	
1275D 40R1 95-104	diabase	Pl, Amp/Cpx/Chl	185.1					609					

[a] Sample: hole-core-section-cm interval; δ^{34}S in per mil VCDT; AVS, acid-volatile sulfide; CRS, chromium-reduced sulfide; SO_4, sulfate-sulfur; Pl, plagioclase; Amp, amphibole; Cpx, clinopyroxene; Ilm, ilmenite; Qz, quartz; Serp, serpentine; Bru, brucite; Mt, magnetite; Iwa, iowaite; Ol, olivine; Opx, orthopyroxene.
[b] Total S as determined by CHN analyzer.

Finally, δ^{18}O values of 6.1–8.1‰ for 6 serpentinites from Hole 1272A are consistently enriched in ^{18}O compared to fresh mantle peridotite.

[20] Gabbroic rocks cored during Leg 209 are generally depleted in ^{18}O compared to fresh rock values of 5.7 ± 0.3‰ [*Muehlenbachs and Clayton*, 1972; *Harmon and Hoefs*, 1995]. Twenty gabbros from Site 1275 have consistently low δ^{18}O values of 3.3–4.9‰ (Figures 2 and 4, Table 2). Likewise, four gabbroic rocks from Hole 1270B are depleted in ^{18}O (δ^{18}O = 4.4–5.5‰), and single gabbro samples from Holes 1268A and 1272A have low δ^{18}O values (5.5 and 4.3‰, respectively; Figure 2; Table 2).

4.3. Opaque Mineralogy

[21] The least altered peridotites from Hole 1274A contain relict primary sulfide phases, including pentlandite [$(FeNi)_9S_8$] with variable amounts of chalcopyrite ($CuFeS_2$) and minor bornite (Cu_5FeS_4). These assemblages are replaced by secondary sulfide minerals, alloys, and native metals (awaruite [$FeNi_3$] and native copper). Awaruite and heazlewoodite (Ni_3S_2) are the most common replacement products, surrounding or intergrown with pentlandite (Figures 5a and 5b), and magnetite commonly mantles pentlandite and awaurite. These textures document desulfurization of primary sulfides during serpentinization under reducing conditions [e.g., *Alt and Shanks*, 1998; *Bach et al.*, 2004a]. Secondary hydrothermal sulfides are rare and include small grains of valleriite [4(FeCuNi)S-3(MgFeAl)$(OH)_2$] and pyrite (FeS_2) associated with cross-cutting lizardite-chrysotile veinlets.

[22] Primary mantle sulfide minerals are rare in the highly altered peridotites from Hole 1272A, and typically consist of pentlandite grains, mostly altered to heazlewoodite and mantled by awaruite and magnetite. Tiny (<1 μm) secondary pyrite grains are commonly associated with lizardite-chrysotile veins.

[23] Primary mantle sulfides are not preserved in Hole 1268A. The initial serpentinization stage resulted in formation of serpentine and magnetite, with common sulfide minerals in the host rock along sulfide-bearing veinlets and gabbroic dikes. Three types of sulfide/oxide veins are present. The first consists of zoned, massive sulfide-oxide veins containing millerite (NiS) partly altered to polydymite (Ni_3S_4), in turn mantled by euhedral pyrite and magnetite, which are altered to goethite (Figure 5c). This assemblage is also observed in the host rock where millerite is transformed to violarite ($FeNi_2S_4$) + magnetite + hematite (Figure 5d). The second vein type comprises pyrite-talc veins (Figure 5e) that in some cases grade into massive pyrite veins. The third vein type consists of pentlandite + chalcopyrite + pyrite with serpentine. Rocks affected by the later stage talc replacement generally lack sulfide minerals. Earlier vein sulfide minerals in these rocks are altered to Fe-oxides and

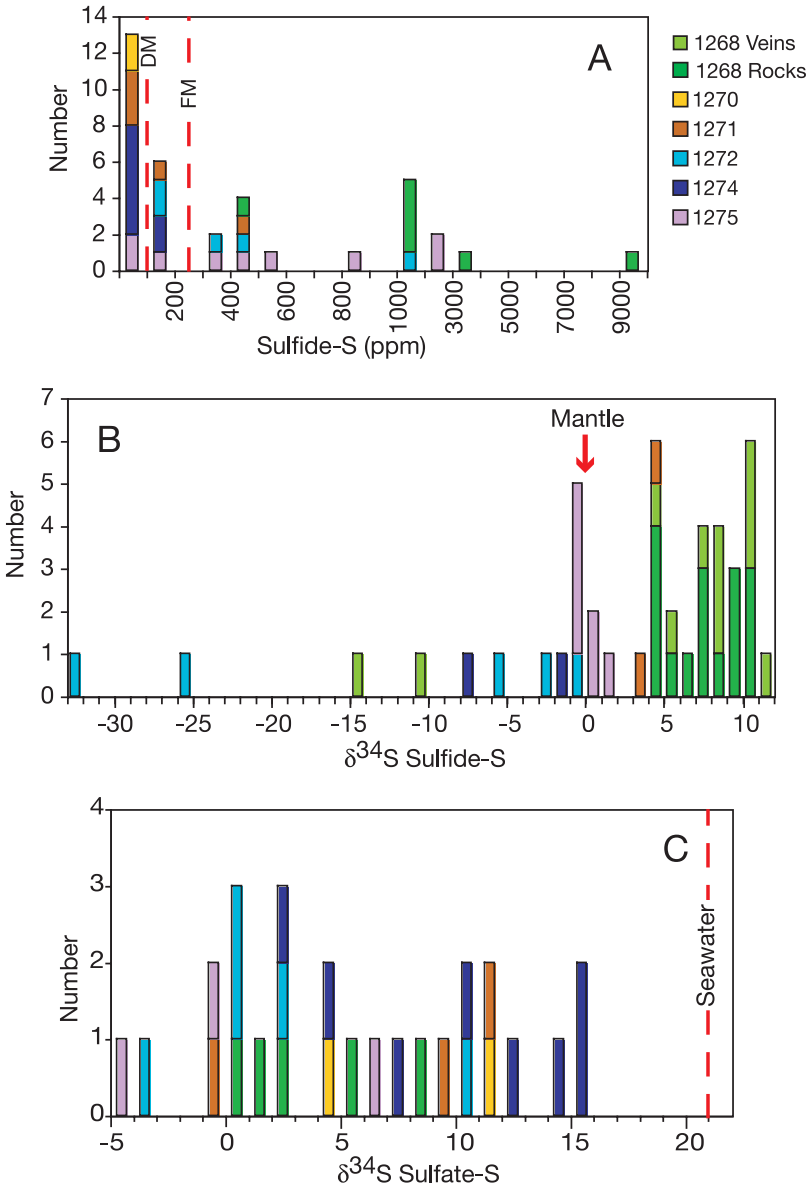

Figure 3. Histograms of bulk rock sulfide-S contents and sulfur isotope compositions of Leg 209 rocks. Data from Table 1. Note scale change in Figure 3a at sulfide-S content of 1000 ppm. Fertile mantle (FM) peridotites contain ~250 ppm sulfur [*Lorand*, 1991; *Hartmann and Wedepohl*, 1992], and removal of 15–20% basalt melt that contains 1000 ppm sulfur will leave depleted mantle (DM) having 60–120 ppm S.

hydroxides during talc alteration, and similar oxidation reactions likely occurred in the host rocks.

5. Discussion

5.1. Petrographic Constraints

[24] Previous work on serpentinized peridotites from Leg 209 by *Bach et al.* [2004a] documents two major reaction pathways. Tremolite and talc replace pyroxene during higher temperature reactions, >350–400°C, where olivine is stable and alteration of pyroxene maintains low pH and high silica activity in solution. At temperatures <250°C, pyroxene reaction is sluggish and olivine reacts rapidly to serpentine + magnetite + brucite. In this case pH increases and silica activity is low. In both cases, once the more rapidly reacting phase is exhausted, interaction of fluid with the residual phase changes fluid pH and silica activity such that brucite or talc react to form serpentine, leading to completely altered rocks that contain serpentine + magnetite, but little or no brucite or talc.

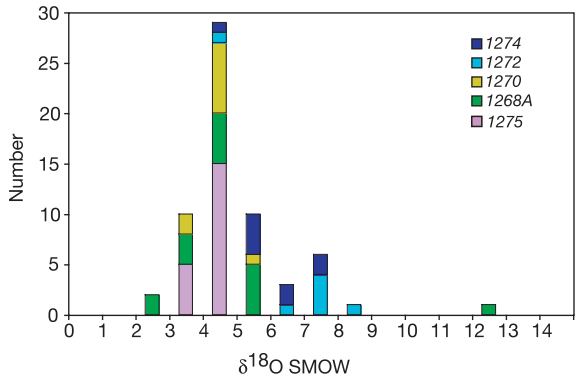

Figure 4. Histogram of bulk rock oxygen isotope compositions for Leg 209 rocks. Data from Table 2.

[25] At Site 1268, serpentinites underwent a subsequent replacement by talc as the result of silica metasomatism by fluids derived from seawater-gabbro interaction or by breakdown of pyroxene deeper in the basement [*Bach et al.*, 2004a; *Paulick et al.*, 2006]. All sites underwent late, low-temperature seafloor alteration to varying degrees, with oxidation of the rocks and formation of carbonate veins [*Bach et al.*, 2004a]. Iowaite also formed during late oxidation in serpentinites at Site 1272.

5.2. Oxygen Isotopes

[26] The bulk rock oxygen isotope data are used here to provide constraints on the temperatures of alteration and serpentinization. The serpentinites are highly recrystallized and reasonable assumptions can be made about fluid-rock isotope fractionation, but fluid compositions can vary, so this effect is also discussed. A convenient approach is to use the water-rock interaction calculations of *Taylor* [1977]. The water/rock ratio is given by the following formula:

$$(W/R)_A = (\delta_r^f - \delta_r^i)/(\delta_w^i - \delta_w^f),$$

where $(W/R)_A$ is the atomic water/rock ratio, δ_r^i and δ_r^f are the initial and final rock $\delta^{18}O$ values, respectively, and δ_w^i and δ_w^f are the initial and final fluid $\delta^{18}O$ values. Figure 6 shows examples of these calculations assuming the initial fluid is seawater (0‰), initial peridotite has the composition of pristine mantle (5.5‰ [*Mattey et al.*, 1994]), and that the oxygen isotope fractionation between bulk rock and fluid is equivalent to the temperature dependent fractionation between serpentine and water given by P. J. Saccocia et al. (Oxygen and hydrogen isotope fractionation in the serpentine-water and talc-water systems from 250° to 450°C, manuscript in preparation, 2007; hereinafter referred to as Saccocia et al., manuscript in preparation, 2007) (see Figure 6). Besides serpentine, the rocks also contain magnetite, brucite and talc, but the presence of small amounts of these phases does not significantly change the results of the water/rock ratio calculations. The presence of 5% magnetite or brucite would lower the calculated rock $\delta^{18}O$ values or increase the fluid $\delta^{18}O$ by <0.8‰, and the presence of talc would have an opposite effect [*Wenner and Taylor*, 1971; *Saccocia et al.*, 1998; Saccocia et al., manuscript in preparation, 2007].

[27] For a seawater starting fluid, serpentinized peridotites are depleted in ^{18}O and fluids are correspondingly enriched in ^{18}O at temperatures above 200°C, whereas at lower temperatures the rocks are enriched in ^{18}O (Figure 6). At temperatures of 250–350°C, water/rock ratios of 0.1–1 produce serpentinite having $\delta^{18}O$ of ~2–5‰, similar to values observed at Sites 1268 and 1270 and locally in Hole 1274A. If seawater is the reacting fluid, the bulk rock ^{18}O-enrichments observed in Hole 1272A ($\delta^{18}O$ up to 8.1‰) and locally in Holes 1274A and 1268A ($\delta^{18}O = 7–12$‰) require lower temperatures, less than ~150°C.

[28] Fluid compositions are not well constrained, however, and seawater fluids that had previously interacted with peridotite could be involved. At temperatures of 250–400°C seawater reacting with peridotite at low water/rock ratios (~1–0.1) results in ^{18}O-enriched fluids, having $\delta^{18}O$ values of ~1–6‰ (Figure 6). A reacted seawater fluid having $\delta^{18}O$ = 3‰ could produce the ^{18}O-depleted serpentinites having $\delta^{18}O$ ~3–5‰ at water/rock ratios of ~1 (Figure 7). The presence of relict olivine and orthopyroxene at Site 1270 and in Hole 1274A, along with the presence of early formed talc and brucite, suggest low water/rock ratios at these sites [*Bach et al.*, 2004a].

[29] Serpentinization at lower temperatures, below ~200°C, produces fluids depleted in ^{18}O compared to seawater (Figure 6). If the ^{18}O-enriched serpentinites in Hole 1272A and locally in Holes 1274A and 1268A formed by reaction with such evolved seawater fluids, then temperatures of serpentinization for these rocks were less than those estimated for seawater fluids. For example, serpentine having $\delta^{18}O$ values of 8–12‰ would be in equilibrium with a fluid having $\delta^{18}O$ = −4 to −6‰ at 80–130°C (Saccocia et al., manuscript in preparation, 2007). Alteration temperatures in peridotites ranged down to values of ~10°C at least locally

Table 2. Bulk Rock Oxygen Isotope Data for Leg 209 Rocks[a]

Hole	Core	Sc	Cm Interval	Rock Type	Depth, mbsf	$\delta^{18}O$	Alteration[b]	Deformation
1268A	2	1	10–14	harz	14.10	5.9	Talc/Serp/	
1268A	2	2	108–115	harz	16.48	3.7	Serp//Talc	
1268A	3	1	29–38	harz	20.49	12.1	Talc//	
1268A	4	1	26–32	harz	25.06	3.6	Serp//Talc	
1268A	4	3	26–35	harz	28.04	4.8	Talc//	
1268A	8	1	28–35	harz	44.28	5.9	Talc//	
1268A	10	1	58–64	harz	54.18	5.0	Talc//	
1268A	11	1	78–85	harz	59.38	5.6	Talc/Serp/	
1268A	13	1	46–55	harz	68.66	4.1	Serp/Talc/	
1268A	17	2	131–138	dunite	90.21	4.4	Serp//	
1268A	18	3	100–110	harz	95.59	4.6	Talc//Serp	
1268A	19	1	34–43	harz	97.34	3.4	Serp//Talc	
1268A	19	3	6–13	dunite	99.88	2.9	Serp//	
1268A	20	2	121–127	harz	104.24	4.4	Talc//	
1268A	24	2	13–20	harz	122.18	2.6	Serp//	
1268A	28	2	7–14	ox gab-nor	141.49	5.5	Talc, Amp/Amp Veins	
1270B	1	1	120–128	ox gab	1.2	4.6	Green Amp/Veins	ductile
1270B	3	1	43–50	ox gab	17.83	4.5	Green Amp/Veins	ductile
1270B	4	2	44–52	ox gab	19.44	4.4	Green Amp/Veins	ductile
1270B	7	1	18–22	harz	31.68	4.8	Talc//	
1270B	8	2	122–128	ox gab	39.08	4,7	Green Amp/Veins	ductile
1270C	2	1	40–46	harz	12.90	4.0	Serp/Talc, Opx/Mt?	
1270C	3	1	12–15	harz	18.62	4.1	Serp/Talc, Opx/Mt?	
1270D	1	1	69–73	harz	0.69	5.2	Serp/Talc/Opx, Mt	
1270D	3	2	39–47	harz	20.55	4.9	Serp/Talc/Mt	
1270D	6	1	58–63	harz	33.48	3.2	Serp/Talc/Mt	
1272A	4	1	110–124	gab-diorite	23.5	4.3	high-T amp	ductile
1272A	13	2	14–21	harz	62.34	7.3	Serp/Iwa	
1272A	16	1	82–89	harz	75.82	7.6	Serp/Iwa	
1272A	21	1	27–37	harz	99.17	7.5	Serp, Iwa	
1272A	24	1	104–112	harz	114.54	8.1	Serp, Iwa	
1272A	26	1	50–57	harz	123.50	6.1	Serp, Iwa/Bru	
1272A	26	3	59–68	harz	125.82	7.1	Serp/Iwa, Ol/Mt	
1274A	3	1	111–120	harz	18.01	6.4	Serp/Ol, Bru/Mt	
1274A	6	2	128–135	harz	32.73	5.8	Serp/Opx, Ol, Bru/	
1274A	10	1	3–19	dunite	49.93	7.4	Serp/Bru/Ol	
1274A	14	1	30–36	harz	69.30	7.4	Serp, Opx/Bru/Ol, Mt	
1274A	16	1	44–52	dunite	84.14	6.0	Serp//Bru, Ol, Mt	
1274A	17	1	121–129	harz	89.51	4.8	Serp/Opx/Bru,Mt	
1274A	18	1	83–93	harz	94.13	5.4	Serp, Opx//Bru, Mt, Ol?	
1274A	22	1	24–32	harz	122.34	5.7	Serp, Opx/Ol/Bru, Mt, Iwa	
1274A	27	2	5–11	harz	147.65	5.4	Serp/Ol/Bru/Opx	
1275B	4	1	70–78	ox gab	18.7	3.3	green amp	
1275B	10	3	24–33	ox gab	49.93	3.6	green Amp/Felsic Veins	
1275B	12	1	105–114	ox gab	57.35	4.7	dk green amp veins	
1275B	16	2	52–59	ox gab	77.42	4.4	green amp	
1275B	18	2	75–84	ox gab	86.92	4.9	Wall rock of felsic- dk green amp vein	
1275B	20	2	118–128	ox gab	96.74	4.7	felsic + dk green Amp Vein	
1275B	22	2	23–33	ox gab	105.73	4.2	lt green veins	
1275D	7	1	96–104	ox gab	33.06	4.0	green amp/felsic patches	
1275D	9	1	49–59	troct	42.09		amp-chl	
1275D	15	2	11–21	ox gab	71.82	4.7	green amp/felsic veins	
1275D	18	1	122–132	ox gab	85.62	3.9	green amp/no veins	
1275D	19	2	31–43	ox gab	91.15	4.2	felsic + dk green amp	
1275D	22	1	97–104	ox gab	104.67	4.7	green amp/no veins	

Table 2. (continued)

Hole	Core	Sc	Cm Interval	Rock Type	Depth, mbsf	$\delta^{18}O$	Alteration[b]	Deformation
1275D	23	1	91–96	ol gab	106.41	4.2	green amp/no veins	
1275D	26	1	60–72	ox gab	118.8	4.3	green amp/no veins	
1275D	35	1	90–100	ox gab	161.7	3.9	green amp	
1275D	36	1	74–79	ox gab	166.54	4.3	green amp	
1275D	38	2	44–53	ox gab	177.18	4.6	green amp/dk green veins	
1275D	40	2	121–131	ox gab	186.75	4.3	green amp	
1275D	43	1	106–116	ox gab	200.36	4.0	green amp	
1275D	43	4	22–31	ox gab	204.02	3.9	green amp	

[a] Sc, section; $\delta^{18}O$ in ‰ VSMOW. Abbreviations: Amp, amphibole; Serp, serpentine; Bru, brucite; Opx, orthopyroxene; Mt, magnetite; Iwa, iowaite; Ol, olivine; lt, light; dk, dark; harz, harzburgite; gab, gabbro; nor, norite; ox, oxide; troct, troctolite.
[b] Alteration of peridotites based on X-ray diffraction (University of Bonn). Abundance of mineral phases estimated on the basis of relative peak heights: major/minor/trace. Alteration of gabbroic rocks given as major secondary phases/vein type based on thin section petrography.

along fractures, as indicated by oxygen isotope compositions of late carbonate veins associated with Fe-oxyhydroxides [*Bach et al.*, 2004b].

[30] Chlorite and amphibole are the dominant alteration phases in gabbroic rocks from Leg 209, requiring alteration of the rocks at temperatures above ~200–300°C. Because of the small mineral-water oxygen isotope fractionations for these phases at temperatures of 200–400°C [*Wenner and Taylor*, 1971; *Bottinga and Javoy*, 1975], the low $\delta^{18}O$ values of the gabbros indicate alteration by seawater-dominated hydrothermal fluids.

[31] Thus petrographic constraints given above discriminate peridotite alteration reactions at temperatures above ~350°C from those occurring below ~250°C, and oxygen isotope data help separate peridotite alteration into reactions occurring at temperatures above 200°C and those below 200°C, down to less than 100°C. Late carbonate veins formed at seafloor alteration temperatures of ~10°C [*Bach et al.*, 2004b]. The mineralogy and oxygen isotope compositions of gabbros indicate that, although low temperature alteration effects may be present, the rocks dominantly reflect alteration at temperatures above ~200°C. These criteria provide a useful framework for interpretation of the sulfur data and for understanding processes of alteration affecting the upper mantle and lower crustal rocks from the 15°20′N area.

5.3. Low-Temperature Reactions in Holes 1272A and 1274A

[32] As discussed above, the consistent bulk rock ^{18}O-enrichments of serpentinite in Hole 1272A (Figures 2 and 4) reflect alteration at temperatures below ~150°C. The serpentinites have relatively high sulfide-S contents compared to depleted peridotites (up to 1980 ppm versus ~100 ppm), and have negative sulfide $\delta^{34}S$ values (−0.3 to −32.1‰). Sulfate contents are high (680–1620 ppm) and sulfate $\delta^{34}S$ values are low relative to that of seawater sulfate (−3.0 to 10.2‰ versus ~22‰ [*Ding et al.*, 2001; *Rees et al.*, 1978]). At temperatures of 50–150°C, the equilibrium fractionation between sulfate and sulfide in solution should be ~40–60‰ [*Ohmoto and Goldhaber*, 1997], whereas that between sulfate and sulfide in the Hole 1272A rocks is only ~1–36‰ (Table 1; Figure 8). The higher values could possibly reflect equilibrium, but the origin of the low $\delta^{34}S$ values of the sulfate (2–10‰) still require explanation. In the past such low $\delta^{34}S$ values of bulk rock sulfate have been attributed to oxidation of low-$\delta^{34}S$ sulfide minerals in the rocks and mixing of this with seawater sulfate, present in pore fluids or as a sulfate mineral [e.g., *Alt and Shanks*, 1998, 2003]. We favor this interpretation for the Leg 209 rocks as well. The local presence of iron oxyhydroxides in Leg 209 rocks is consistent with oxidation occurring near the seafloor, but oxidation could also have taken place during storage of rock samples or sample powders. Assuming that the low $\delta^{34}S$ values of sulfate result from oxidation of sulfide minerals in the rocks, the sulfide contents can be corrected for this by mass balance, yielding higher sulfide-S contents of ~500–3000 ppm.

[33] At the low temperatures of peridotite alteration in Hole 1272A, inorganic reduction of sulfate is kinetically inhibited, and the high pH during serpentinization further inhibits inorganic sulfate reduction [*Ohmoto and Lasaga*, 1982; *Chiba and Sakai*, 1985; *Ohmoto and Goldhaber*, 1997]. Hydrogen produced by serpentinization is a potential reductant for sulfate, but experiments using H_2 did not produce measurable reduction of sulfate at

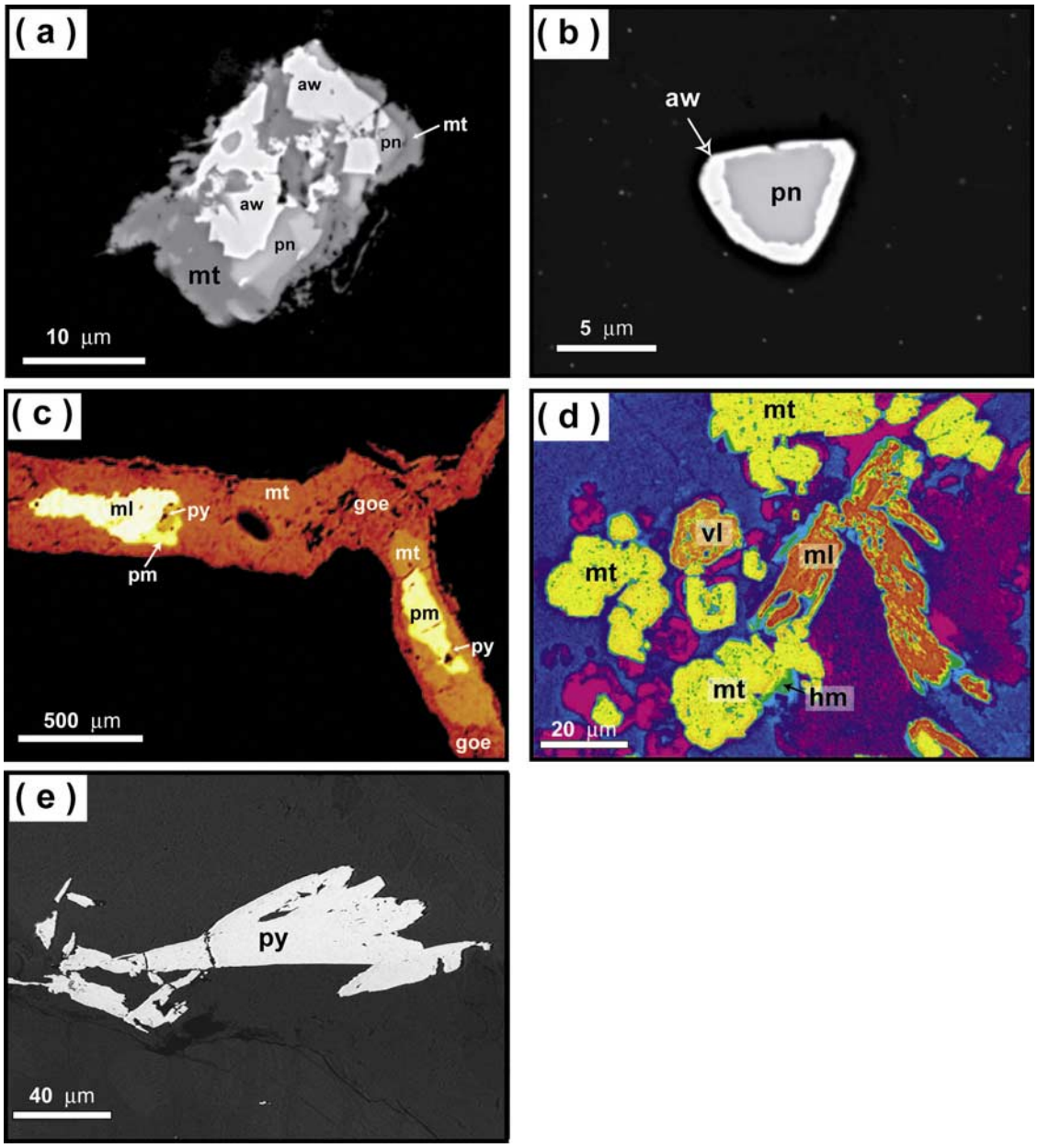

Figure 5. Back-scattered electron images of representative sulfides, oxides, and native metal assemblages in variably serpentinized peridotite samples from ODP Leg 209. (a) Grain of magmatic pentlandite partly altered to awaruite, both mantled by late magnetite along a lizardite-magnetite veinlet (Sample 1274A-1R1-40-46). (b) Euhedral grain of magmatic pentlandite inclusion in olivine, partly replaced by a corona of awaruite, in partly serpentinized harzburgite (Sample 1274A-8R1-72-82). (c) Massive sulfide-oxide vein in serpentinized harzgburgite from (Sample 1268A-13R1-46-55). The vein center consists of millerite, partly transformed to polydymite and mantled by euhedral pyrite and magnetite, which, in turn, is variably altered to spongy Fe oxy-hydroxides. (Gray scale transformed to color-indexed scale to improve contrast among phases.) (d) Sulfide and oxide minerals in serpentinized harzburgite (Sample 1268-20R1-8-12). Euhedral crystals of millerite are partly altered to violarite, and both are mantled by magnetite and late hematite. (BSE gray scale transformed to color-indexed image and color scaled to improve the contrast among phases.) (e) Pyrite in pyrite-talc vein within serpentinized harzburgite (Sample 1268A-15R4-011-15). Pyrite is pseudomorphic after an unknown phase, probably replacing millerite or pyrrhotite. All images were obtained with a Zeiss FEG-SEM at the CIC of the University of Granada (Spain). (aw, awaruite, $FeNi_3$; goe, goethite, FeOOH; hm, hematite, Fe_2O_3; ml, millerite, NiS, mt, magnetite, Fe_3O_4; pn, pentlandite, $(Fe,Ni)_9S_8$; pm, polydymite, Ni_3S_4; py, pyrite; vl, violarite, $FeNi_2S_4$.)

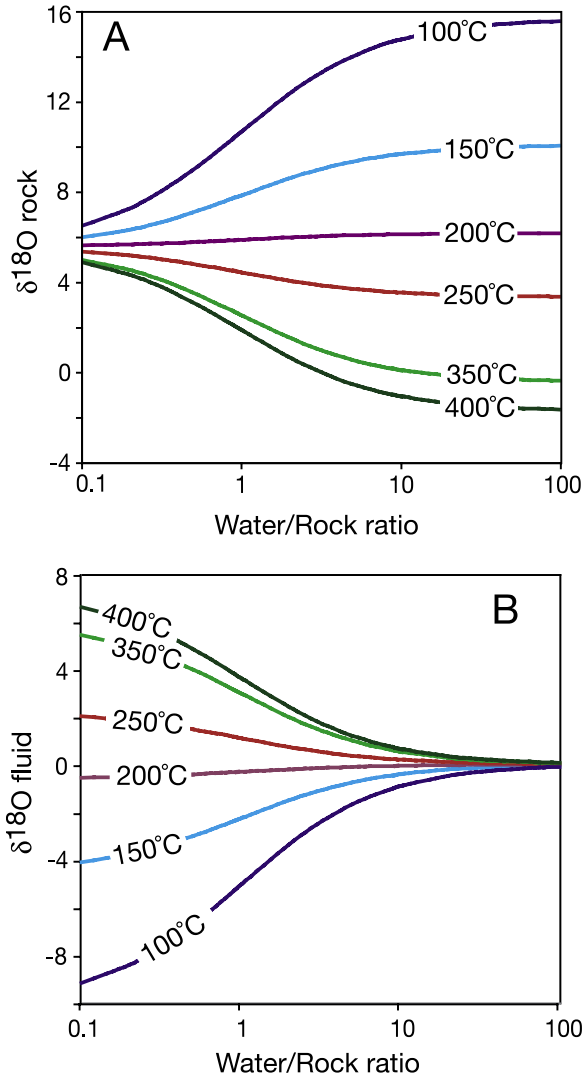

Figure 6. Examples of the effects of seawater interaction with peridotite on the oxygen isotope compositions of (a) rock and (b) fluid, using the water/rock calculations of *Taylor* [1977]. Altered rocks are enriched in ^{18}O at temperatures <200°C and depleted in ^{18}O at higher temperatures. See text for formula details and discussion. Initial fluid $\delta^{18}O = 0‰$, initial peridotite $\delta^{18}O = 5.5‰$, and peridotite-water isotope fractionation assumed equal to that of serpentine-water experimentally determined at 250–450°C by Saccocia et al. (manuscript in preparation, 2007): $1000\ln\alpha = 3.49 \times 10^6\ T^{-2} - 9.48$. W/R_A is atomic water/rock ratio for a closed system and is twice that of the water/rock mass ratio. $\delta^{18}O$ values are shifted to slightly lower W/R for an open system, where $W/R_{open\ system} = \ln [1 + W/R_{closed\ system}]$.

temperatures below 275°C [*Malinin and Khitarov*, 1969]. *Ohmoto and Goldhaber* [1997], however, cite experiments suggesting that sulfate reduction by H_2 may occur at ~200°C if catalyzed by surface reactions. This suggests the possibility that sulfate reduction by H_2 at relatively low temperatures may be catalyzed by metal alloys in serpentinized peridotites. Although awaruite is present in Hole 1272A, metal alloys are extremely rare in serpentinite at the Iberian Margin, the one site where the effects of low-temperature sulfate reduction during serpentinization are well documented [*Alt and Shanks*, 1998]. This suggests that if such reactions were important at that site, they must have occurred early at low water/rock ratios. Thus, in the absence of any convincing evidence that inorganic reduction of sulfate is likely at these low temperatures, we interpret the elevated sulfide-S contents and negative $\delta^{34}S_{sulfide}$ values of the serpentinites from Hole 1272A to result from addition of sulfide produced by microbial reduction of seawater sulfate. Although the net fractionation produced by microbial sulfate reduction varies depending on such factors as temperature, the specific rate of reduction, the electron donor, the concentration of sulfate, and the amount of disproportionation and oxidation of intermediate sulfur species, the bulk rock sulfide $\delta^{34}S$ values for Hole 1272A are similar to those for biogenic sedimentary pyrite [*Canfield*, 2002].

[34] Serpentinization produces hydrogen via oxidation of ferrous iron to magnetite [e.g., *Moody*, 1976; *Frost*, 1985] (see discussions by *Alt and*

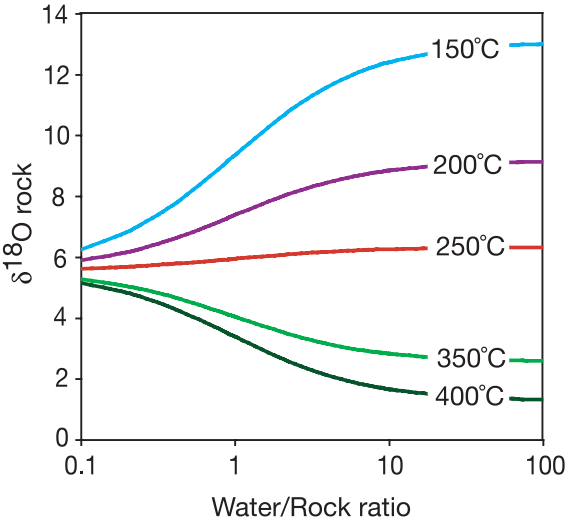

Figure 7. Fluid oxygen isotope compositions for reactions of peridotite starting material ($\delta^{18}O = 5.5‰$) with ^{18}O-enriched hydrothermal fluid ($\delta^{18}O = 3‰$) at varying temperatures and water/rock ratios [after *Taylor*, 1977] (see text for details). W/R_A is atomic water/rock ratio for a closed system.

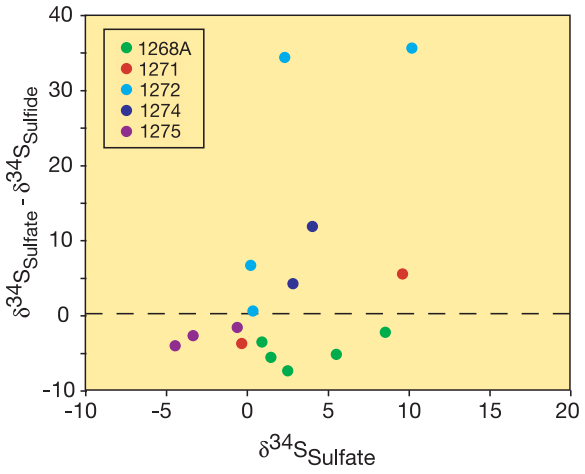

Figure 8. Fractionation of sulfur isotopes between bulk rock sulfate and sulfide versus δ^{34}S of sulfate from Leg 209 rocks. Low δ^{34}S of sulfate and low $\delta^{34}S_{sulfate} - \delta^{34}S_{sulfide}$ results from oxidation of sulfide minerals in the rocks. Negative values for $\delta^{34}S_{sulfate} - \delta^{34}S_{sulfide}$ may result from kinetic fractionation during oxidation or possibly from oxidation of sulfide derived from microbial reduction of seawater sulfate. See text for discussion.

Shanks [1998] and *Bach et al.* [2006]). Hydrogen is the principal electron donor in anoxic and carbon-starved environments [*Jannasch*, 1995] and is the most likely electron donor for sulfate reduction in the serpentinites. Much of the sulfide added to the rocks may reside in the fine (submicrometer) pyrite and valleriite along serpentine veins.

[35] The ^{18}O enrichments of serpentinites in Hole 1274A occur in the upper half of the hole (Figure 2, Table 2) and suggest alteration by seawater at relatively low (less than ~150°C) temperatures. This is consistent with the mineralogy of the rocks, where replacement of olivine by lizardite and brucite (±magnetite) and the presence of fresh clinopyroxene within completely serpentinized olivine indicate relatively low temperatures of serpentinization (<200–250°C [*Bach et al.*, 2004a]). The upper 90 m of the core is also affected by late, low-temperature alteration and formation of Fe-oxyhydroxides and carbonates, and further silicate alteration under these conditions could contribute to the bulk rock ^{18}O enrichments. Local whole rock ^{18}O depletions in the lower portion of the hole suggest higher temperatures of alteration, above 200°C. Sulfide-S contents of rocks from Hole 1274A are generally low (<160 ppm), but assuming that low δ^{34}S values for sulfate (2.8–15.3‰) result from oxidation of sulfide minerals in the rocks, then corrected sulfide-S contents are ~310–860 ppm, enriched relative to depleted peridotite (~100 ppm). Only two samples contained sufficient sulfide-S for isotope analysis, but these have negative values, as low as −7.5‰ (Table 1). These negative δ^{34}S values, the recalculated high sulfide-S contents, and the low temperatures of serpentinization all indicate that microbial sulfate reduction was important at this site. Although early alteration may have occurred at temperatures too high to support life, the oxygen and sulfur isotope compositions of the rocks reflect the effects of lower-temperature alteration and microbial sulfate reduction. *Bach et al.* [2006] show that magnetite formation in Leg 209 serpentinites is relatively late. Thus much of the hydrogen production through formation of magnetite occurred relatively late, possibly at lower temperatures conducive to biological activity. As in Hole 1272A, much of the low δ^{34}S sulfide may reside in the very fine-grained disseminated pyrite.

5.4. High-Temperature Reactions in Hole 1268A

[36] The characteristic bulk rock ^{18}O-depletions in Hole 1268A (Figures 2 and 4) indicate that alteration took place at generally high temperatures, in the range of 200°C–400°C. Because of the difference in mineral-water oxygen isotope fractionation, talc-rich rocks from Hole 1268A have slightly higher δ^{18}O than serpentine-rich rocks (mostly 4.6–5.9‰ versus 2.6–4.4‰, respectively; Figure 2, Table 2), but estimates of temperatures and fluid S and O isotope compositions are similar. Serpentinized peridotites from Hole 1268A are enriched in LREE and have positive Eu anomalies [*Paulick et al.*, 2006]. The similarity of the REE patterns of the serpentinites to those of high-temperature (~350°C) hydrothermal fluids venting from peridotite outcrops on the MAR suggested to these authors that the peridotites were altered by similar hydrothermal fluids, consistent with the temperature estimates from oxygen isotopes.

[37] Total sulfur contents of rocks from Hole 1268A in Table 1 are high (0.1–1.4 wt%), consistent with previously reported S contents (0.1–2.1 wt% S [*Paulick et al.*, 2006]). Bulk rock sulfide-S has uniformly high δ^{34}S values (4.4–10.8‰; mean = 8.4‰), and eleven vein pyrites have similar high δ^{34}S values (4.6–10.8‰; mean = 8.3‰; two other vein pyrites, discussed in the following section, have negative values; Figures 2 and 3, Table 1). The high sulfide-S contents and elevated δ^{34}S

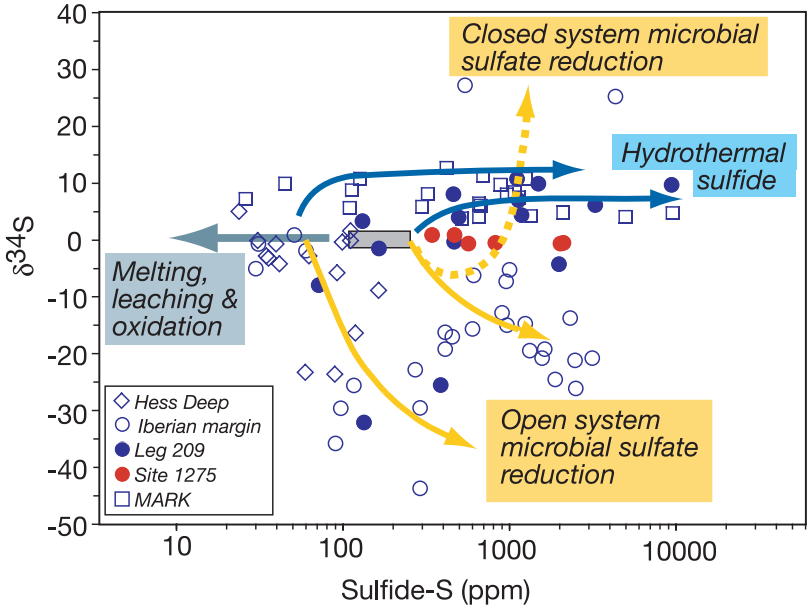

Figure 9. Summary figure showing serpentinization processes affecting oceanic peridotites. Removal of basaltic melts, hydrothermal leaching, and seafloor oxidation results in loss of sulfur with no isotope fractionation, but oxidation of sulfide minerals contributes to low δ^{34}S for sulfate. Hydrothermal serpentinization and talc alteration lead to isotope exchange and addition of ^{34}S-enriched hydrothermal sulfide to the rocks, as shown schematically by the two curves. Serpentinization at low temperatures supports microbial sulfate reduction, which leads to elevated S contents and low δ^{34}S values. Lines indicate potential pathways for addition of sulfide from open-system microbial reduction of seawater sulfate (using $\alpha_{\text{sulfate-sulfide}}$ = 1.04–1.06, typical for biogenic sedimentary pyrite [*Canfield*, 2002]). Closed-system sulfate reduction can lead to elevated δ^{34}S values, as shown by the dashed curve showing progressive addition of 1000 ppm sulfide via closed-system (Rayleigh fractionation) reduction of seawater sulfate. The δ^{34}S of sulfide in Iberian margin serpentinites increases with depth, from −15 to −30‰ near the surface to +25–27‰ at ~150 m, reflecting a change from open to more closed conditions with depth [*Alt and Shanks*, 1998]. Depending upon isotope fractionation and openness of the system to seawater, pathways for addition of seawater-derived sulfide to the rocks can lie between the open and closed end-members. Data from Table 1 and *Alt and Shanks* [1998, 2003]. Sulfide in gabbros from Site 1275 mainly reflects magmatic variations in sulfur content with little variation in isotope composition.

values are consistent with alteration by upwelling hydrothermal fluids. These results are similar to those for serpentinized peridotites from the MARK area [*Alt and Shanks*, 2003], where geochemical modeling shows that the high sulfide-S contents and elevated δ^{34}S values of the rocks cannot be acquired by reaction of peridotite with seawater, and could only be acquired through a 2-stage alteration process. Initially, seawater reacted with gabbro at elevated temperatures (>350°C) where sulfide minerals are unstable and sulfide is leached from the rocks. In addition, seawater sulfate is reduced to sulfide, producing a sulfide-bearing, high-δ^{34}S hydrothermal fluid. This fluid then reacted with peridotite at lower temperatures (<350°C), precipitating sulfide minerals in the rocks and resulting in the strong S- and ^{34}S-enrichments of the serpentinites. Prior reaction of seawater with gabbro is required because prior reaction with peridotite does not produce sufficient sulfur metasomatism and leaves significant (~25 wt%) olivine in the metasomatized serpentinite, in contrast to the observed near-complete alteration [*Alt and Shanks*, 2003]. Sulfur and oxygen isotope data, bulk rock chemistry, and mineralogy all indicate that similar processes occurred at Site 1268 (Tables 2 and 3) [*Bach et al.*, 2004a; *Paulick et al.*, 2006].

[38] Talc alteration is superimposed on serpentinization in Hole 1268A as the result of silica metasomatism by hydrothermal fluids. Consequently, the rocks gained SiO_2 and REE, and lost H_2O as talc replaced serpentine [*Bach et al.*, 2004a; *Paulick et al.*, 2006]. Talc alteration also resulted in a slight increase in δ^{18}O of the rocks (Table 2). The 2 talc-altered peridotites from Hole 1268A in Table 1 have total S contents lower than the 5 serpentinites, suggesting loss of sulfur during talc alteration. This

is supported by data from *Paulick et al.* [2006]: 12 talc altered peridotites from Hole 1268A contain an average of 0.34 wt% total S (±0.27; range = 0.10–0.88 wt%), whereas 25 serpentinites average 0.59% S (±0.51; range = 0.12–2.09 wt%). The sulfide mineralogy indicates a change from sulfide formation during serpentinization to oxidation of sulfides during talc alteration as the reducing capacity of the system is exhausted [*Bach et al.*, 2006]. The source of the silica bearing fluid has been suggested to be underlying gabbros and/or harzburgite undergoing hydrothermal alteration at temperatures >350°C, where pyroxene in harzburgite breaks down leading to higher Si activity in solution [*Bach et al.*, 2004a; *Paulick et al.*, 2006].

[39] Local bulk rock ^{18}O-enrichments in Hole 1268A (up to 12.1‰) result from low-temperature (<150°C) alteration. This is consistent with the local presence in the cores of iron oxyhydroxides and carbonates, both products of late, low-temperature alteration at temperatures down to ~2–15°C [*Bach et al.*, 2004a, 2004b]. Most pyrite veins in Hole 1268A have high δ^{34}S values identical to those for sulfide in bulk rocks (~5–11‰), but 2 veins have significantly different, negative values of −11.7 and −15.2‰ (Table 1, Figure 2). These data suggest that, although high-temperature hydrothermal processes dominate in Hole 1268A, microbial reduction of seawater sulfate occurred after the basement cooled to low temperatures.

[40] As discussed above for Hole 1272A, the low δ^{34}S values of sulfate are generally interpreted to reflect a mixture of seawater sulfate with sulfate derived from oxidation of low δ^{34}S sulfide minerals in the rocks [e.g., *Alt and Shanks*, 1998, 2003]. Sulfate in Hole 1268A, however, has δ^{34}S values that are lower than coexisting sulfide-S in the rocks (Figures 2 and 8). One possibility is that this results from a kinetic isotope fractionation during oxidation of sulfide minerals. Depending on the oxidation mechanism, kinetic fractionation can occur if dissolved sulfide, intermediate sulfoxyanions, or some *Thiobacillus* species are present [*Toran and Harris*, 1989; *Ohmoto and Goldhaber*, 1997]. Another possibility is that a sulfide component having even lower δ^{34}S values, like those of the 2 vein pyrites, was oxidized. There could be a sulfide component derived from microbially reduced seawater sulfate in the rocks that is more readily oxidized than the hydrothermal sulfide minerals. The microbially produced sulfide minerals may be finer grained and hence more reactive and susceptible to oxidation. Similar effects are observed in one sample from Site 1271 and three samples from Site 1275 (Figure 8, Table 1). Both cases suggest the possibility that microbial activity may be involved, either in sulfate reduction or sulfide oxidation.

5.5. Sites 1270 and 1271

[41] Serpentinites from shallow (<60 m) holes at Site 1270 exhibit consistent bulk rock ^{18}O-depletions, suggesting serpentinization by seawater-derived fluids at temperatures greater than ~200°C, and consistent with the occurrence of talc and tremolite, which indicate higher temperature alteration (>350°C [*Bach et al.*, 2004a]). The mineralogy and ^{18}O-depletions of gabbroic rocks from Hole 1270B also indicate alteration at temperatures above ~200°C. Only two serpentinite samples from Site 1270 were analyzed for S contents, and both have very low sulfide-S contents (Table 1). These samples are from depths <24 mbsf, and the low S contents reflect oxidation of sulfide minerals and loss of S from the rocks during late, low-temperature alteration near the seafloor, as evidenced by the presence of Fe-oxyhydroxides.

[42] No oxygen isotope data are available for Site 1271, but the sulfur data provide some constraints on alteration processes. Two samples from the shallow portion of Hole 1271A (<30 m) contain no detectable sulfide-S (Table 1). These cores were affected by low temperature seafloor alteration and oxidation, which resulted in oxidation of sulfide minerals and loss of sulfur from the rocks.

[43] In contrast, two samples from >60 m in Hole 1271B have relatively high sulfide-S contents and elevated δ^{34}S values (up to ~500 ppm and 3.3–4.0‰; Table 1). These data suggest addition of hydrothermal sulfide to the rocks, similar to processes affecting rocks in Hole 1268A. In addition, peridotites in this portion of the hole are characterized by impregnation and infiltration by mafic melts that experienced syn-deformational hydrothermal alteration to amphibolite, and peridotites associated with these ampibolites contain amphibole and talc, consistent with high-temperature (>350°C) alteration. The sulfur data suggest that amphibolitizing or later hydrothermal fluids contained hydrothermal sulfide similar to that in Hole 1268A, consisting of sulfide derived from leaching of gabbro or peridotite at high temperature (~0‰) mixed with sulfide derived from inorganic reduction of seawater sulfate (~22‰) at high temperatures, similar to the hydrothermal fluids that affected Hole 1268A.

5.6. Gabbros and Troctolites at Site 1275

[44] The secondary mineralogy and ^{18}O depletions of gabbroic rocks from Site 1275 indicate alteration by seawater hydrothermal fluids at temperatures above ~200–300°C. Gabbros and troctolites in Holes 1275B and D have variable sulfide-sulfur contents, 15–2110 ppm (Table 1), with this variation generally reflecting magmatic processes. Troctolites have the lowest S contents, consistent with their origin as dunites impregnated with basaltic melts [*Kelemen et al.*, 2004]. The highest sulfide-S contents (~2000 ppm; Table 1) correspond to oxide-rich gabbros, which concentrate sulfur through differentiation and enrichment of iron and sulfur [e.g., *Alt and Anderson*, 1991]. Sulfide-S has $\delta^{34}S$ values of −0.7 to 1.3‰ (Table 1, Figures 2 and 3), which scatter about the mantle value (0‰), and the mean value (0.1‰ ± 0.9‰) is indistinguishable from mantle sulfide. Thus, despite alteration over a range of conditions from amphibolite and greenschist grades to low-temperatures and recrystallization of igneous sulfide minerals, the sulfide-sulfur in these rocks is primary. The lack of significant alteration effects on sulfur in the rocks may be attributed to low water/rock ratios for each alteration stage, with rock-dominated sulfur in solution, such that sulfide contents and $\delta^{34}S$ values are little changed from igneous values.

[45] As at the other sites, sulfate in Site 1275 gabbroic rocks has low $\delta^{34}S$ values indicating that it is derived largely from oxidation of low-$\delta^{34}S$ sulfide minerals in the rocks. The sulfate in Site 1275 rocks has very low $\delta^{34}S$ values, however, down to −4.5‰, even lower than the $\delta^{34}S$ of associated sulfide-S (Table 1, Figure 8). As discussed for Hole 1268A, this may reflect a kinetic isotope fractionation during oxidation of sulfide minerals, or oxidation of a low-$\delta^{34}S$ sulfide component produced by microbial activity. Conditions were appropriate as indicated by the common evidence for late water-rock interactions at low-temperatures. Basaltic oceanic basement has been shown to harbor microbial activity [*Furnes and Staudigel*, 1999], including sulfate reducing organisms [*Alt et al.*, 2003], but the sulfate data presented here suggest that gabbroic basement may also support microbial activity where conditions are conducive.

6. Summary and Conclusions

[46] Sulfur and oxygen isotope data for serpentinized and talc-altered peridotites and for altered gabbroic rocks from the area of the 15°20′N Fracture Zone on the MAR provide information about hydrothermal alteration processes, fluid compositions, and the presence of a subsurface biosphere in oceanic basement. Three general processes are identified and shown schematically in Figure 9. These include (1) high-temperature hydrothermal alteration with addition of high-$\delta^{34}S$ sulfide to the rocks; (2) low-temperature (<150°C) alteration supporting microbial sulfate reduction and addition of low-$\delta^{34}S$ sulfide to the rocks; and (3) low-temperature seafloor alteration reactions leading to oxidation and loss of sulfide-sulfur from the rocks.

[47] Serpentinized peridotites from Hole 1268A are characterized by ^{18}O depletions (2.6–4.4‰) resulting from high-temperature (~250–350°C) hydrothermal processes. Serpentinization resulted in formation of pyrite in rocks and veins, and elevated whole rock sulfide-S contents and $\delta^{34}S$ values (up to ~2 wt% and 4.4–10.8‰). Fluids were derived from high-temperature (>350°C) reaction of seawater with gabbro at depth. Subsequent silica metasomatism resulting in talc alteration of serpentinized peridotite produced slight bulk rock ^{18}O enrichments (mostly 4.6–5.9‰). Similar hydrothermal processes produced elevated sulfide-S contents and $\delta^{34}S$ values locally at Site 1271.

[48] Elevated $\delta^{18}O$ values for rocks from Holes 1272A and 1274A (up to 8.1‰) result from low-temperature (<150°C) serpentinization reactions. These supported microbial activity, most likely through generation of hydrogen during serpentinization. Microbial reduction of seawater sulfate resulted in addition of low-$\delta^{34}S$ sulfide to rocks, producing elevated sulfide-S contents, up to ~3000 ppm, and negative $\delta^{34}S$ values, down to −32.1‰. This process also occurred locally at other sites, as evidenced by negative $\delta^{34}S$ of some vein pyrites from Hole 1268A.

[49] Serpentinites from Site 1270 are depleted in ^{18}O reflecting high-temperature serpentinization reactions, but sulfide-S contents are low as the result of late oxidation and sulfur loss near the seafloor.

[50] Gabbroic rocks and troctolites from Site 1275 are significantly altered over a wide range of conditions, yet $\delta^{34}S$ values of sulfide-S are indistinguishable from primary magmatic values and sulfide-S contents mainly reflect magmatic processes.

[51] Sulfate extracted from bulk rocks at all sites typically has low $\delta^{34}S$ values that reflect oxidation

of sulfide minerals in the rocks. Sulfate having lower $\delta^{34}S$ than associated sulfide-S may reflect a kinetic isotope effect during oxidation of sulfide minerals, or could result from oxidation of a sulfide phase(s) having very low (negative) $\delta^{34}S$ produced by microbial sulfate reduction at low temperatures.

[52] The processes of serpentinization around the 15°20′ Fracture Zone documented in this work are generally similar to those described elsewhere, leading to some generalizations about controls on serpentinization processes. First, the Leg 209 peridotite sections affected by higher temperature alteration, as indicated by whole rock ^{18}O-depletions, contain gabbroic rocks or impregnations by mafic melts (Sites 1268, 1270, and 1271). Similar associations of gabbroic rocks and high-temperature serpentinization occur at the MARK area. The involvement of gabbros in generating serpentinizing fluids appears to be a common process, and the association of gabbroic material and high temperature serpentinization suggests that heat from mafic melts may commonly be important in serpentinization. Second, the Leg 209 drill holes are all sited on fault surfaces, but lower temperature alteration of peridotites occurs in those sections that penetrate faults at depth (tectonic mega-breccia and fault in Hole 1272A, faults in Hole 1274A). A similar association of faulting and low-temperature serpentinization occurs at the Iberian Margin, where drilling of exposed mantle penetrated a tectonic mega-breccia. These associations suggest that faulting not only leads to unroofing and exposure of mantle material but also that faulting contributes to significant cooling and affects the style of serpentinization. Such low-temperature serpentinization (<150°C) supports microbial reduction of seawater sulfate, and this is a common process in mantle exposed at the seafloor. Finally, low temperature oxidation effects are mainly related to late fracturing and proximity to the seafloor.

Acknowledgments

[53] The authors thank Mike Mottl, two anonymous reviewers, and associate editor Bill Seyfried for helpful comments that led to improvements to this paper. J.A.'s contribution was supported by NSF OCE 0424558. H.P. received funding for this research from the German Research Foundation (DFG). H.P. thanks J. Hoefs and R. Przybilla for help and advice during laser measurements at the University of Göttingen. G.B. acknowledges a Natural Sciences and Engineering Council of Canada Discovery grant. This research used samples and/or data provided by the Ocean Drilling Program. The ODP is sponsored by the U.S. National Science Foundation (NSF) and participating countries under the management of Joint Oceanographic Institutions (JOI).

References

Agrinier, P., R. Hekinian, D. Bideau, and M. Javoy (1995), O and H stable isotope compositions of oceanic crust and upper mantle rocks exposed in the Hess Deep near the Galapagos Triple Junction, *Earth Planet. Sci. Lett.*, *136*, 183–196.

Agrinier, P., G. Cornen, and M. O. Beslier (1996), Mineralogical and oxygen isotope features of serpentinites recovered from the ocean/continent transition in the Iberia Abyssal Plain, *Proc. Ocean Drill. Program Sci. Results*, *149*, 541–552.

Allen, D. E., and W. E. J. Seyfried (2003), Compositional controls on vent fluids from ultramafic-hosted hydrothermal systems at mid-ocean ridges: An experimental study at 400°C, 500 bars, *Geochim. Cosmochim. Acta*, *67*(8), 1531–1542.

Allen, D. E., and W. E. J. Seyfried (2004), Serpentinization and heat generation: Constraints from Lost City and Rainbow hydrothermal systems, *Geochim. Cosmochim. Acta*, *68*(6), 1347–1354.

Alt, J. C., and T. F. Anderson (1991), The mineralogy and isotopic composition of sulfur in Layer 3 gabbros from the Indian Ocean, ODP Hole 735B, *Proc. Ocean Drill. Program Sci. Results*, *118*, 113–125.

Alt, J. C., and W. C. Shanks (1998), Sulfur in serpentinized oceanic peridotites: Serpentinization processes and microbial sulfate reduction, *J. Geophys. Res.*, *103*, 9917–9929.

Alt, J. C., and W. C. Shanks (2003), Serpentinization of abyssal peridotites from the MARK area, Mid-Atlantic Ridge: Sulfur geochemistry and reaction modeling, *Geochim. Cosmochim. Acta*, *67*, 641–653.

Alt, J. C., G. J. Davidson, D. A. H. Teagle, and J. A. Karson (2003), The isotopic composition of gypsum in the Macquarie Island ophiolite: Implications for the sulfur cycle and the subsurface biosphere in oceanic crust, *Geology*, *31*, 549–552.

Bach, W., N. R. Banerjee, H. J. B. Dick, and E. T. Baker (2002), Discovery of ancient and active hydrothermal systems along the ultra-slow spreading Southwest Indian Ridge 10°–16°E, *Geochem. Geophys. Geosyst.*, *3*(7), 1044, doi:10.1029/2001GC000279.

Bach, W., C. J. Garrido, H. Paulick, J. Harvey, and M. Rosner (2004a), Seawater-peridotite interactions: First insights from ODP Leg 209, MAR 15°N, *Geochem. Geophys. Geosyst.*, *5*, Q09F26, doi:10.1029/2004GC000744.

Bach, W., H. Paulick, and Ocean Drilling Program Leg 209 Shipboard Scientific Party (2004b), C and O isotope composition of carbonates from serpentinites at the Mid-Atlantic Ridge, 14 to 16°N, Ocean Drilling Program Leg 209, paper presented at 27th European Geosciences Union General Assembly, Nizza, France.

Bach, W., H. Paulick, C. J. Garrido, B. Ildefonse, W. P. Meurer, and S. E. Humphris (2006), Unraveling the sequence of serpentinization reactions: petrography, mineral chemistry, and petrophysics of serpentinites from MAR 15°N (ODP Leg 209, Site 1274), *Geophys. Res. Lett.*, *33*, L13306, doi:10.1029/2006GL025681.

Barnes, J. D., and Z. D. Sharp (2006), A chlorine isotope study of DSDP/ODP serpentinized ultramafic rocks: Insights into the serpentinization process, *Chem. Geol.*, *228*, 246–265.

Bottinga, Y., and M. Javoy (1975), Oxygen isotope partitioning among the minerals and triplets in igneous and metamorphic rocks, *Rev. Geophys.*, *13*, 401–418.

Bougault, H., J. L. Charlou, Y. Fouquet, H. D. Needham, N. Vaslet, P. Apprious, P. J. Baptiste, P. A. Rona, L. Dimitriev, and S. Silantev (1993), Fast and slow spreading ridges: Structure and hydrothermal activity, ultramafic topographic highs and CH_4 output, *J. Geophys. Res.*, *98*, 9643–9651.

Canfield, D. E. (2002), Biogeochemistry of sulfur isotopes, in *Stable Isotope Geochemistry*, *Rev. Mineral.*, vol. 43, edited by J. W. Valley and D. R. Cole, pp. 607–633, Mineral. Soc. of Am., Washington, D. C.

Canfield, D. E., R. Raiswell, J. T. Westrich, C. M. Reaves, and R. A. Berner (1986), The use of chromium reduction in the analysis of reduced inorganic sulfur in sediments and shales, *Chem. Geol.*, *54*, 149–155.

Carbotte, S., and D. S. Scheirer (2004), Variability of ocean crustal structure created along the global mid-ocean ridge, in *Hydrogeology of the Oceanic Lithosphere*, edited by E. E. Davis and H. Elderfield, pp. 59–107, Cambridge Univ. Press, Cambridge, U. K.

Charlou, J. L., Y. Fouquet, H. Bougault, J. P. Donval, J. Etoubleau, J. Jean-Baptiste, A. Dapoigny, P. Appriou, and P. A. Rona (1998), Intense CH_4 plumes generated by serpentinization of ultramafic rocks at the intersection of the 15°20′N fracture zone and the Mid-Atlantic Ridge, *Geochim. Cosmochim. Acta*, *62*, 2323–2333.

Chiba, H., and H. Sakai (1985), Oxygen isotope exchange rate between dissolved sulfate and water at hydrothermal temperatures, *Geochim. Cosmochim. Acta*, *49*, 993–1000.

Clayton, R. N., and T. K. Mayeda (1963), The use of bromide pentafluoride in the extraction of oxygen from oxides and silicates for isotopic analysis, *Geochim. Cosmochim. Acta*, *27*, 43–52.

Coplen, T. B., and H. R. Krouse (1998), Sulphur isotope data consistency improved, *Nature*, *392*(6671), 32.

Davis, A. S., D. S. Clague, R. A. Zierenberg, C. G. Wheat, and B. L. Cousens (2003), Sulfide formation related to changes in the hydrothermal system on Loihi seamount, Hawai'i, following the seismic event in 1996, *Can. Mineral.*, *41*, 457–472.

Ding, T., S. Valkiers, H. Kipphardt, P. De Bi`Evre, P. D. P. Taylor, R. Gonfiantini, and R. Krouse (2001), Calibrated sulfur isotope abundance ratios of three IAEA sulfur isotope reference materials and V-CDT with a reassessment of the atomic weight of sulfur, *Geochim. Cosmochim. Acta*, *65*, 2433–2437.

Douville, E., J. L. Charlou, E. H. Oelkers, P. Bianvenu, C. F. Jove Colon, J. P. Donval, Y. Fouquet, D. Prieur, and P. Appriou (2002), The rainbow vent fluids (36°14′N, MAR): The influence of ultramafic rocks and phase separation on trace metal contents on Mid-Atlantic Ridge hydrothermal fluids, *Chem. Geol.*, *184*, 37–48.

Escartín, J., C. Mével, C. J. MacLeod, and A. M. McCaig (2003), Constraints on deformation conditions and the origin of oceanic detachments: The Mid-Atlantic Ridge core complex at 15°45′N, *Geochem. Geophys. Geosyst.*, *4*(8), 1067, doi:10.1029/2002GC000472.

Frost, B. R. (1985), On the stability of sulfides, oxides and native metals in serpentine, *J. Petrol.*, *26*, 31–63.

Fruh-Green, G. L., A. Plas, and C. Lecuyer (1996), Petrologic and stable isotopic constraints on hydrothemal alteration and serpentinization of the EPR shallow mantle at Hess Deep, Site 895, *Proc. Ocean Drill. Program Sci. Results*, *147*, 109–163.

Fujiwara, T., J. Lin, T. Matsumoto, P. B. Kelemen, B. E. Tucholke, and J. F. Casey (2003), Crustal evolution of the Mid-Atlantic Ridge near the Fifteen-Twenty Fracture Zone in the last 5 Ma, *Geochem. Geophys. Geosyst.*, *4*(3), 1024, doi:10.1029/2002GC000364.

Furnes, H., and H. Staudigel (1999), Biological mediation in ocean crust alteration: How deep is the deep biosphere?, *Earth Planet. Sci. Lett.*, *166*, 97–103.

Harmon, R. S., and J. Hoefs (1995), Oxygen isotope heterogeneity of the mantle deduced from global ^{18}O systematics of basalts from different geotectonic settings, *Contrib. Mineral. Petrol.*, *120*(1), 95–114.

Hartmann, G., and K. H. Wedepohl (1992), The composition of peridotite tectonites from the Ivrea Complex, northern Italy: Residues from melt extraction, *Geochim. Cosmochim. Acta*, *57*, 1761–1782.

Jannasch, H. W. (1995), Microbial interactions with hydrothermal fluids, in *Seafloor Hydrothermal Systems*, *Geophys. Monogr. Ser.*, vol. 91, edited by S. E. Humphris et al., pp. 273–296, AGU, Washington, D. C.

Kelemen, P. B., et al. (Eds.) (2004), *Proceedings of the Ocean Drilling Program, Initial Reports* [online], vol. 209, Ocean Drill. Program, College Station, Tex. (Available at http://www-odp.tamu.edu/publications/209_IR/209ir.htm)

Kelley, D. S., et al. (2001), An off-axis hydrothermal vent field near the mid-Atlantic ridge at 30°N, *Nature*, *412*, 145–149.

Kelley, D. S., et al. (2005), A serpentinite-hosted ecosystem: The Lost City Hydrothermal Field, *Science*, *307*, 1428–1434.

Lagabrielle, Y., D. Bideau, M. Cannat, J. A. Karson, and C. Mével (1998), Ultramafic-mafic plutonic rock suites exposed along the Mid-Atlantic Ridge (10°N–30°N)—Symmetrical asymmetrical distribution and implications for seafloor spreading processes, in *Faulting and Magmatism at Mid-Ocean Ridges*, *Geophys. Monogr. Ser.*, vol. 106, edited by W. R. Buck et al., pp. 153–176, AGU, Washington, D. C.

Lorand, J. P. (1991), Sulphide petrology and sulphur geochemistry of orogenic lherzolites: A comparative study of the Pyrenean bodies (France) and the Lanzo Massif (Italy), in *Orogenic Lherzolites and Mantle Processes*, edited by M. A. Menzies et al., pp. 77–95, Oxford Univ., London.

Malinin, S. D., and N. I. Khitarov (1969), Reduction of sulfate sulfur by hydrogen under hydrothermal conditions, *Geochem. Int.*, *6*(6), 1022–1027.

Mattey, D., and C. Macpherson (1993), High-precision oxygen isotope microanalysis of ferromagnesian minerals by laser-fluorination, *Chem. Geol.*, *105*, 305–318.

Mattey, D., D. Lowry, and C. Macpherson (1994), Oxygen isotope composition of mantle peridotite, *Earth Planet. Sci. Lett.*, *128*, 231–241.

Mevel, C. (2003), Serpentinization of abyssal peridotites at mid-ocean ridges, *C. R. Geosci.*, *335*, 825–852.

Moody, J. B. (1976), An experimental study on the serpentinization of iron bearing olivines, *Can. Mineral.*, *14*, 462–478.

Muehlenbachs, K., and R. N. Clayton (1972), Oxygen isotope studies of fresh and weathered submarine basalts, *Can. J. Earth Sci.*, *9*, 172–184.

Ohmoto, H., and M. B. Goldhaber (1997), Sulfur and carbon isotopes, in *Geochemistry of Hydrothermal Ore Deposit*, edited by H. L. Barnes, pp. 517–612, John Wiley, New York.

Ohmoto, H., and A. C. Lasaga (1982), Kinetics of reactions between aqueous sulfates and sulfides in hydrothermal systems*Geochim. Cosmochim. Acta*, *46*, 1727–1745.

Palandri, J. L., and M. H. Reed (2004), Geochemical models of metasomatism in ultramafic systems: Serpentinization, rodingitization, and sea floor carbonate chimney precipitation, *Geochim. Cosmochim. Acta*, *68*, 1115–1133.

Paulick, H., W. Bach, M. Godard, J. C. M. De Hoog, G. Suhr, and J. Harvey (2006), Geochemistry of abyssal peridotites (Mid-Atlantic Ridge, 15°20′N, ODP Leg 209): Implications for fluid/rock interaction in slow spreading environments, *Chem. Geol.*, *234*, 179–210.

Proskurowski, G., M. D. Lilley, D. S. Kelley, and E. J. Olson (2006), Low temperature volatile production at the Lost City Hydrothermal Field: Evidence from a hydrogen stable isotope geothermometer, *Chem. Geol.*, *229*, 331–343.

Rees, C. E., W. J. Jenkins, and J. Monster (1978), The sulphur isotopic composition of ocean water sulphate, *Geochim. Cosmochim. Acta*, *42*, 337–381.

Rice, C. A., M. L. Tuttle, and R. L. Reynolds (1993), The analysis of forms of sulfur in ancient sediments and sedimentary rocks: Comments and cautions, *Chem. Geol.*, *107*, 83–95.

Saccocia, P. J., J. S. Seewald, and W. C. Shanks (1998), Hydrogen and oxygen isotope fractionation between brucite and aqueous NaCl solutions from 250 to 450°C, *Geochim. Cosmochim. Acta*, *62*, 485–492.

Seyfried, W. E., Jr., D. I. Foustoukos, and D. E. Allen (2004), Ultramafic-hosted hydrothermal systems at mid-ocean ridges: Chemical and physical controls on pH, redox carbon reduction reactions, in *Mid-Ocean Ridges: Hydrothermal Interactions Between the Lithosphere and Oceans*, *Geophys. Monogr. Ser.*, vol. 148, edited by C. R. German, J. Lin, and L. M. Parson, pp. 267–284, AGU, Washington, D. C.

Seyler, M., J. P. Lorand, H. J. B. Dick, and M. Drouin (2007), Pervasive melt percolation reactions in ultra-depleted refractory harzburgites at the Mid-Atlantic Ridge, 15 degrees 20′N: ODP Hole 1274A, *Contrib. Mineral. Petrol.*, *153*, 303–319.

Sharp, Z. D. (1990), A laser-based microanalytical method for the in situ determination of oxygen isotope ratios of silicates and oxides, *Geochim. Cosmochim. Acta*, *54*, 1353–1357.

Taylor, H. P. (1977), Water/rock interactions and the origin of H_2O in granitic batholiths, *J. Geol. Soc. London*, *133*, 509–558.

Toran, L., and R. F. Harris (1989), Interpretation of sulfur and oxygen isotopes in biological and abiological sulfide oxidation, *Geochim. Cosmochim. Acta*, *53*, 2341–2348.

Valley, J. W., N. E. Kitchen, M. J. Kohn, C. R. Niendorf, and M. J. Spicuzza (1995), UWG-2, a garnet standard for oxygen isotope ratio: Strategies for high precision and accuracy with laser heating, *Geochim. Cosmochim. Acta*, *59*, 5223–5231.

Wenner, D. B., and H. P. Taylor (1971), Temperatures of serpentinization of ultramafic rocks based on $^{18}O/^{16}O$ fractionation between coexisting serpentine and magnetite, *Contrib. Mineral. Petrol.*, *32*, 165–185.